Evidence for a continuous decline in lower stratospheric ozone offsetting ozone layer recovery

William T. Ball[1,2], Justin Alsing[3,4], Daniel J. Mortlock[4,5,6], Johannes Staehelin[2],
Joanna D. Haigh[4,7], Thomas Peter[2], Fiona Tummon[2], Rene Stübi[8],
Andrea Stenke[2], John Anderson[9], Adam Bourassa[10], Sean M. Davis[11,12],
Doug Degenstein[10], Stacey Frith[13,14], Lucien Froidevaux[15], Chris Roth[10],
Viktoria Sofieva[16], Ray Wang[17], Jeannette Wild[18,19], Pengfei Yu[11,12],
Jerald R. Ziemke[14,20], and Eugene V. Rozanov[1,2]

[1]Physikalisch-Meteorologisches Observatorium Davos World Radiation Centre, Dorfstrasse 33, 7260 Davos Dorf, Switzerland
[2]Institute for Atmospheric and Climate Science, Swiss Federal Institute of Technology Zurich, Universitaetstrasse 16, CHN, CH-8092 Zurich, Switzerland
[3]Center for Computational Astrophysics, Flatiron Institute, 162 5th Ave, New York, NY 10010, USA
[4]Physics Department, Blackett Laboratory, Imperial College London, SW7 2AZ, UK
[5]Department of Mathematics, Imperial College London, SW7 2AZ, UK
[6]Department of Astronomy, Stockholms universitet, SE-106 91 Stockholm, Sweden
[7]Grantham Institute - Climate Change and the Environment, Imperial College London, SW7 2AZ, UK
[8]Federal Office of Meteorology and Climatology, MeteoSwiss, CH-1530 Payerne, Switzerland
[9]Hampton University, Hampton, VA, USA
[10]Institute of Space and Atmospheric Studies, University of Saskatchewan, Saskatoon, Canada
[11]Cooperative Institute for Research in Environmental Sciences, University of Colorado, Boulder, CO, USA
[12]NOAA Earth System Research Laboratory, Boulder, CO, USA
[13]NASA Goddard Space Flight Center, Silver Spring, MD, USA
[14]Science Systems and Applications Inc., Lanham, MD, USA
[15]Jet Propulsion Laboratory, California Institute of Technology, Pasadena, CA, USA
[16]Finnish Meteorological Institute, Helsinki, Finland
[17]School of Earth and Atmospheric Sciences, Georgia Institute of Technology, Atlanta, GA, USA
[18]NOAA/NWS/NCEP/Climate Prediction Center, College Park, MD, USA
[19]Innovim LLC, Greenbelt, MD, USA
[20]NASA Goddard Space Flight Center, Greenbelt, MD, USA

Correspondence to: W. T. Ball (william.ball@env.ethz.ch)

Abstract. Ozone forms in the Earth's atmosphere from the photodissociation of molecular oxygen, primarily in the tropical stratosphere. It is then transported to the extratropics by the Brewer-Dobson circulation (BDC), forming a protective 'ozone layer' around the globe. Human emissions of halogen-containing ozone-depleting substances (hODSs) led to a decline in stratospheric ozone until they were banned by the Montreal Protocol (MP), and since 1998 ozone in the upper stratosphere shows a likely recovery. Total column ozone measurements of ozone between the Earth's surface and the top of the atmosphere, indicate that the ozone layer has stopped declining across the globe, but no clear increase has been observed at latitudes outside the polar regions (60°–90°). Here we report evidence from multiple satellite measurements that ozone in the lower stratosphere between 60°S and 60°N has declined continuously since 1985. We find that, even though upper stratospheric ozone is recovering in response to the MP, the lower stratospheric changes more than compensate for this, resulting in the conclusion that, globally (60°S–60°N), stratospheric column ozone continues to deplete. **We find that globally, total column ozone appears not to have decreased because of likely increases in tropospheric column ozone that compensate for the stratospheric decreases.** The reason for the continued reduction of lower stratospheric ozone is not clear, models do not reproduce these trends, and so the causes now urgently need to be established.

1   Introduction

The stratospheric ozone layer protects surface life from harmful solar ultraviolet radiation. In the second half of the 20th century, halogen-containing ozone depleting substances (hODSs) resulting from human activity, mainly in the form of chloroflurocarbons (CFCs), led to the decline of the ozone layer (Molina and Rowland, 1974). The ozone hole over the South pole was the clearest example of ozone depletion, but total column ozone was declining globally (Farman et al., 1985; WMO/NASA, 1988; WMO, 2011, 2014). The Montreal Protocol came into effect in 1989, banning multiple substances responsible for ozone layer depletion, and by **the mid-2000s it had become apparent that a decline in total column ozone had stopped at almost all non-polar latitudes since around 1997 (WMO, 2006)**.

The general expectation is that global mean stratospheric column ozone will increase as hODSs continue to decline, **but increasing total column ozone due to decreasing ODSs has not yet been reported** (WMO, 2014); a cooling stratosphere is also thought to aid the recovery of ozone by slowing temperature-dependent reaction rates, **and by accelerating ozone transport through the meridional Brewer Dobson Circulation (BDC). Chemistry climate models (CCMs)** predict that mean total column ozone will increase, but this also remains uncertain since projections rely substantially on the CO_2, N_2O and CH_4 emissions scenarios **(Revell et al., 2012; Nowack et al., 2015)**.

Only recently has a total column ozone recovery been detected **over Antarctica** during the austral spring (Solomon et al., 2016). However, non-polar (<60°) global total column ozone levels

have remained stable since 2000 (WMO, 2014), with most latitudes displaying a positive, but non-significant, decadal trend (WMO, 2014). **Results from Frith et al. (2014) and (Weber et al., 2017) suggest a potential peak in positive trends around 2011, after which positive trends decreased, and while uncertainties shrink, significance remains elusive**.

40   Despite a lack of clear recovery in total column ozone, ozone appears to be significantly recovering in the upper stratosphere above 10 hPa in multiple ozone composites that merge observations from various space missions, especially at mid-latitudes (Kyrölä et al., 2013; Laine et al., 2014; WMO, 2014; Tummon et al., 2015; Harris et al., 2015; Steinbrecht et al., 2017; Ball et al., 2017; Frith et al., 2017; Sofieva et al., 2017; Bourassa et al., 2017). Trends are almost always presented

45   as percentage-change per decade, which does not illuminate the contribution to the column ozone changes. Thus, a recovery in upper stratospheric ozone does not mean that stratospheric ozone as a whole is recovering. Indeed, if total column ozone does not display any significant changes since 1997, while the upper stratosphere displays significant increases, then either the uncertainties due to unattributed dynamical variability interfere in the significance of the trend determined through

50   regression analysis, or there are counteracting trends at lower levels of the stratosphere, or in the troposphere.

      Suggestions of a decrease in lower stratospheric ozone have been presented elsewhere (Kyrölä et al., 2013; Gebhardt et al., 2014; Sioris et al., 2014; Nair et al., 2015; Vigouroux et al., 2015). However, it has been difficult to confirm (WMO, 2014; Harris et al., 2015; Steinbrecht et al., 2017)

55   because: (i) ozone is typically integrated over wide latitude bands and/or total column ozone is considered, both of which may lead to cancellation of opposing trends; (ii) large dynamical variability unaccounted for in regression analysis together with shorter timeseries lead to higher uncertainties (Tegtmeier et al., 2013); (iii) below 20 km there are large ozone gradients, with low ozone concentrations close to the tropopause; and (iv) composite-data merging techniques have hindered

60   identification of robust changes (Harris et al., 2015; Ball et al., 2017).

      In addition to only reporting decadal percentage changes, most studies typically do not consider altitudes below 20 km (∼60 hPa), missing stratospheric changes down to 16 km in the tropics (30°S–30°N) or ∼12 km at mid-latitudes (60°–30°), regions that contain a large fraction of, and drive most sub-decadal variability in, total column ozone. **Absolute uncertainties between limb sounding in-**

65   **struments have been reported to be up to ∼10–15% near 16 km (Tegtmeier et al., 2013), which should be accounted for from bias corrections when composites are constructed, but which may also reduce confidence in variability and trends in the lower stratosphere. Nevertheless,** a recent study by Bourassa et al. (2017) extended their analysis of the SAGE-II/OSIRIS ozone composite down to 18 km, where widespread, partially significant, negative ozone trends (1998–2016)

70   can be seen at all latitudes from 50°S to 50°N. Models do predict a future decline in tropical lower stratospheric ozone (Eyring et al., 2010; WMO, 2011), but evidence for recent BDC-driven ozone decreases remain weak, and decreases identified at 32–36 km (near 10 hPa) are largely thought to be

due to high ozone levels over 2000–2003 (WMO, 2014), and so may be an artefact of the analysis period rather than a BDC change.

75   **Finally, issues remain in the attribution and identification of ozone recovery usually performed through multiple linear regression (MLR) analysis that can lead to biased trend estimates (Damadeo et al., 2014; Ball et al., 2017) due to geolocation biases (Sofieva et al., 2014), vertical resolution (Kramarova et al., 2013), and satellite drifts and biases from merging data into composites (WMO, 2014; Tummon et al., 2015; Harris et al., 2015; Ball et al., 2017). Most**

80   **studies consider either piecewise linear trends (PWLT) or the equivalent effective stratospheric chlorine (EESC) proxy to represent the influence of hODSs on long-term ozone changes (Newman et al., 2007). Chehade et al. (2014) and Frith et al. (2014) both concluded that total column ozone trends up to 2012 and 2013, respectively, estimated from PWLT or EESC prior to 1997 agree well, but post-1997 the EESC proxy implies significant and positive increases, while**

85   **PWLT trends are generally smaller and non-significant at most non-polar latitudes. This suggests that post-1997 changes in total column ozone may no-longer be well represented by an EESC regressor. Since PWLT represents the overall trend without any specific physical attribution, the total column ozone may indeed be increasing at a slower rate than EESC estimates suggests, or not at all.**

90   **Here, we quantify the absolute changes in ozone in different regions of the stratosphere and troposphere, and their contributions to total column ozone, at different latitudes and globally, since 1998 using a robust regression analysis approach (section 2.1): dynamical linear modelling (DLM) (Laine et al., 2014; Ball et al., 2017). DLM provides a major step forward by estimating smoothly varying, non-linear background trends, without prescribing an EESC ex-**

95   **planatory variable or restrictive piecewise-linear assumptions. Although this precludes a clear physical attribution, similar to PWLT, it allows for an assessment of how ozone is evolving on decadal and longer timescales and to identify if and when an inflection in ozone occurs. We use updated ozone composites extended to 2015/6 (section 3), and put the DLM results of the longer timeseries in context of previously reported percentage-change trends, usually reported from**

100   **20 km upwards, but here extended down to the tropopause (section 4.1). We then consider the absolute contribution to total column ozone of partial column ozone from the upper, middle, lower, and whole stratosphere (section 4.2), and then the tropospheric contribution (section 4.3). We finally show results from two CCMs in specified dynamics mode (section 4.4), and then in section 5 discuss our findings and conclude.**

2 Methods

2.1 Regression analysis

The standard method to estimate decadal trends or changes in ozone, multiple linear regression (MLR), is known to have estimator bias and regressor aliasing (Marsh and Garcia, 2007; Chiodo et al., 2014). To minimise these effects we use a more robust method using a Bayesian inference approach through Dynamical Linear Modelling (DLM) (Laine et al., 2014; Ball et al., 2017; see Laine et al., 2014 for a detailed description of the DLM model and implementation). DLM is similar to MLR in that the same regressors (see section 2.2, below) are used for known drivers of ozone variability, and an autoregressive term is included. However, the trend is not predetermined with a linear, or piecewise-linear, model, but is allowed to smoothly vary in time, and the degree of trend non-linearity is an additional free parameter to be jointly inferred from the data. We infer posterior distributions on the non-linear trends by Markov Chain Monte Carlo (MCMC) sampling; the background trend levels at every month are included as free parameters, with a data-driven prior on the smoothness of the month-to-month trend variability. DLM analyses have more principled uncertainties than MLR since they are based on a more flexible model, and formally integrate over uncertainties in the regression coefficients, (non-stationary) seasonal cycle, autoregressive coefficients and parameters characterizing the degree of non-linearity in the trend. The time-varying, background changes are inferred, rather than specified by, for example, an estimate of equivalent effective stratospheric chlorine (EESC) (Newman et al., 2007) or PWLT; there is no need for assumptions about when and where a decline in hODSs occurs.

2.2 Regressor variables

Similar to MLR, we use regressor timeseries that represent known drivers of stratospheric ozone variability. These include: the 30 cm radio flux (F30) as a solar proxy (as it better represents UV variability than the commonly used F10.7 cm flux (Dudok de Wit et al., 2014)), a latitudinally resolved stratospheric aerosol optical depth (SAOD) for volcanic eruptions (Thomason et al., 2017), an ENSO index (NCAR, 2013) representing El niño Southern Oscillation variability[1], and the Quasi-Biennial Oscillation at 30 and 50 hPa[2]. For total column ozone and partial column ozone trend estimates, we also use the Arctic and Antarctic Oscillation[3] proxy for Northern and Southern . We use a second order autoregressive (AR2) process (Tiao et al., 1990) to avoid the auto-correlation of residuals. We remove the two year period June 1991 to May 1993, inclusive, from the analysis to avoid problems related to impacts of satellite ozone retrieval due to stratospheric aerosol loading

---

[1]From NOAA: http://www.esrl.noaa.gov/psd/enso/mei/table.html

[2]From Freie Universitaet Berlin: http://www.geo.fu-berlin.de/en/met/ag/strat/produkte/qbo/index.html.

[3]From http://www.cpc.ncep.noaa.gov/products/precip/CWlink/daily_ao_index/teleconnections.shtml.

(Davis et al., 2016), and aliasing between regressors within the regression analysis (Chiodo et al., 2014); the volcanic aerosols still show slowly varying changes, which are important to consider as a regressor since this has a larger impact on ozone in the lower stratosphere than the upper.

2.3 Statistics

We do not apply any statistical tests, which therefore avoids making assumptions about the (posterior) distributions. **The posterior distributions that represent the change since January 1998 are formed from the (n=100,000) DLM samples from the MCMC exploration of the model parameters (see section 2.1). Then, probability density functions (PDFs) are estimated as histograms of the sampled DLM changes from 1998. Finally, the probabilities represent the percentage of the posteriors that are negative; therefore, the posteriors and probabilities presented in all figures represent the full information about the change in ozone since 1998 obtained from the DLM analysis; these are not always normally distributed.** Positive increases have values less than 50% and therefore increases at 80, 90 and 95% probabilities are indicated by their respective contours in Fig. 1 and A1, and have values less than or equal to 20, 10 and 5% in Figs. 2, A3, A4, A6, A9, and A10.

3 Ozone Data

3.1 Satellite ozone composites

A summary of the ozone merged datasets – SWOOSH (Davis et al., 2016), GOZCARDS (Froidevaux et al., 2015), SBUV-MOD (Frith et al., 2017), SBUV-Merged-Cohesive (Wild and Long, 2017), SAGE-II/CCI/OMPS (Sofieva et al., 2017) and SAGE-II/OSIRIS/OMPS (Bourassa et al., 2014) – and an intercomparison of the publicly available data up to 2012 can be found in Tummon et al. (2015); data up to 2016 are available upon request from composite PIs, respectively (see also Steinbrecht et al., 2017). These data are monthly, zonally averaged, homogenised, and bias-corrected ozone datasets. **Nevertheless, merged product uncertainties remain large in the upper-troposphere lower-stratosphere (UTLS) region in merged products, with estimated monthly uncertainties of 3–9% in SAGE-II-CCI-OMPS (Sofieva et al., 2017), and drifts of ~1% per decade in the OSIRIS period of SAGE-II-OSIRIS-OMPS (Bourassa et al., 2017). Although data quality degrades in the UTLS, biases are still removed through the same procedure as other parts of the stratosphere and thought to be done optimally (Sofieva et al., 2014); results agree with studies focused on the tropical UTLS (Sioris et al., 2014). Additional uncertainties remain unquantified, such as those in the SBUV (vertically resolved) composites due to very low resolution in the lower stratosphere (Frith et al., 2017), and uncertainties that result from the unit conversion from number-density to volume mixing ratio in the SWOOSH and GOZCARDS composites that require information about local temperature. We note, however,**

Table 1: List of datasets and coverage considered in this study; some data products cover ranges outside those quoted/used here.

Name	Region	Alt./press. range	Location	Version	Units	Merged?
SBUV-MOD[1]	Total column	0–400 km	Space	v8.6	DU	No
Arosa[1]	Total column	0–400 km	Ground	–	DU	No
SBUV-MOD	Stratosphere	50–1 hPa	Space	v8.6[2]	vmr	Yes[3]
SBUV-Mer. Coh.	Stratosphere	50–1 hPa	Space	LOTUS[2]	vmr	Yes[3]
GOZCARDS	Stratosphere	147–1 hPa	Space	v2.20[2]	vmr	Yes[4]
SWOOSH	Stratosphere	147–1 hPa	Space	v2.6	vmr	Yes[4]
SAGE-II-OSIRIS-OMPS	Stratosphere	13–48 km	Space	LOTUS[2]	n-den	No
SAGE-II-CCI-OMPS[1]	Stratosphere	13–48 km	Space	Sofieva et al. (2017)	n-den	No
OMI/MLS	Troposphere	0–16 km	Space	v9/v4.2	DU	No
WACCM-SD	All	0–120 km	Model	v4	vmr	No
SOCOL-SD	All	0–80 km	Model	v3	vmr	No

[1] All data consider the January 1985–December 2016 period, except SAGE-II-CCI-OMPS (1985–2015), Arosa (1970–2015), and SBUV-MOD total column ozone (1970–2016).

[2] All marked datasets were made available through the SPARC Long-term Ozone Trends and Uncertainties in the Stratosphere (LOTUS) activity; unmarked datasets are publicly available.

[3] SBUV-MOD and SBUV-Merged-Cohesive were merged to form Merged-SBUV using the BASIC algorithm laid out in Ball et al. (2017).

[4] GOZCARDS and SWOOSH were merged to form Merged-SWOOSH/GOZCARDS using the BASIC algorithm laid out in Ball et al. (2017).

that formal definitions and calculations of uncertainties vary between composites and cannot necessarily be directly compared (Harris et al., 2015; Ball et al., 2017).

We consider the period 1985–2016 in all cases, except SAGE-II/CCI/OMPS up to 2015, as it ends in July 2016. We consider the latitudinal range 60°S to 60°N where all composites have lati-
175 tudinal coverage, and from 13 to 48 km in SAGE-II/CCI/OMPS and SAGE-II/OSIRIS/OMPS, the approximately equivalent pressure range of 147–1 hPa that we consider in SWOOSH, GOZCARDS, and Merged-SWOOSH/GOZCARDS, and 50–1 hPa in SBUV-NOAA, SBUV-NASA, and Merged-SBUV. SWOOSH, SBUV-Merged-Cohesive and GOZCARDS have been updated since previous intercomparisons (Tummon et al., 2015; Harris et al., 2015); see Table 1 for more information.
180 GOZCARDS v2.20, used here, includes SAGE-II v7.0 and has a finer vertical resolution than earlier versions. It must be stressed that the resolution of SBUV-instruments below 22 hPa (25 km) is low (McPeters et al., 2013; Kramarova et al., 2013), so linear trends estimated at 25–46 hPa also encompass altitudes lower than those that they formally represent (see section 4 for a discussion on this).

3.2 Merged-SWOOSH/GOZCARDS and Merged-SBUV

SWOOSH and GOZCARDS are composites constructed with similar instrument data (Tummon et al., 2015; Ball et al., 2017), but with different pre-processing and merging techniques; the same is true for SBUV-MOD and SBUV-Merged-Cohesive, which are constructed using nadir-viewing backscatter instruments. The Merged-SWOOSH/GOZCARDS and Merged-SBUV results presented here combine these two pairs of composites, which show slightly different spatial variability (Fig. A1) (Tummon et al., 2015; Harris et al., 2015; Steinbrecht et al., 2017; Frith et al., 2017). Part of the reason is related to offsets and drifts in the data that continue to be one of the largest remaining sources of uncertainty within, and between, ozone composites (Harris et al., 2015; Ball et al., 2017; Frith et al., 2017). These artefacts can be largely accounted for using the BAyeSian Integrated and Consolidated (BASIC) methodology developed by Ball et al. (2017), which we apply to both pairs of data separately; examples of corrected timeseries in the lower stratosphere are given in Fig. A2, and others can be found in Ball et al. (2017). This method also fills data gaps, which is reasonable if they are discontinuous for only a few months. This is true for these datasets, but is not for the SAGE-II/CCI/OMPS and SAGE-II/OSIRIS/OMPS.

3.3 Total column ozone

We use merged SBUV v8.6 (Frith et al., 2014) for comparison of results with total column ozone observations, which are available on a 5° latitude grid from 1970 onwards. We verify the stability of SBUV total column ozone after 1997 by comparing SBUV total column ozone overpass data with the independent Arosa ground measurements, which are available from 1926 to present (Scarnato et al., 2010).

3.4 Tropospheric column ozone

For tropospheric ozone, we consider Aura satellite Ozone Monitoring Instrument and Microwave Limb Sounder (OMI/MLS) tropospheric column ozone measurements, discussed by Ziemke et al. (2006). The tropospheric ozone are estimated through a residual method that derives daily maps of tropospheric column ozone by subtracting MLS stratospheric column ozone from co-located OMI total column ozone. The OMI/MLS data, including data quality and data description, are publicly available[4]. Coverage of the OMI/MLS ozone is monthly (October 2004–present) and at $1°×1.25°$ horizontal resolution, which we have zonally averaged to make comparisons here.

[4]From the NASA Goddard website https://acd-ext.gsfc.nasa.gov/Data_services/cloud_slice/
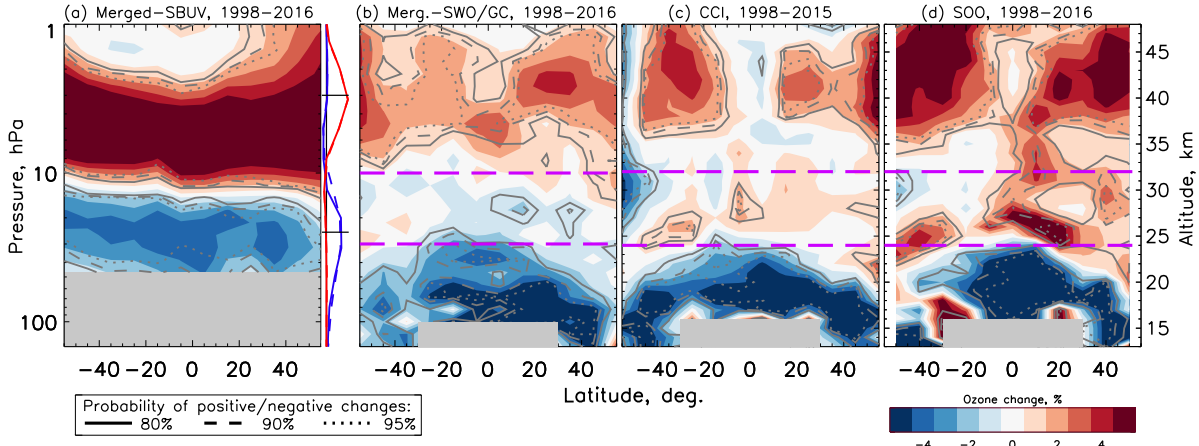
Figure 1: Zonally averaged change in ozone between 1998 and 2016. From (left to right) the Merged-SBUV, Merged-SWOOSH/GOZCARDS, SAGE-II/CCI/OMPS (CCI), and SAGE-II/OSIRIS/OMPS (SOO) composites. Red represents increases, blue decreases (%; see right legend). Contours represent probability levels of positive or negative changes (see left legend). Grey-shaded regions represent unavailable data. Pink dashed-lines delimit regions integrated to partial ozone columns in Figs. 2, A3, A4, A6, A9, and A10. To the right of Merged-SBUV are the instrument observing profiles centred at 3 hPa (red, upper) and 25 hPa (blue) at Northern mid-latitudes (dashed) and in the tropics (solid), from Kramarova et al. (2013). SAGE-II/CCI/OMPS changes are for 1998–2015.

4 Results

4.1 Latitude-altitude resolved post-1997 ozone changes

Concentrations of active stratospheric hODSs reached a maximum in ∼1997 (Newman et al., 2007),
220 and vertically-resolved satellite measurements show evidence that upper stratospheric ozone (10–1 hPa; ∼32–48 km) started recovering soon after (WMO, 2014). Fig. 1 presents post-1998 ozone changes from four ozone composites that combine multiple satellite instruments (see section 3). The Merged-SBUV and Merged-SWOOSH/GOZCARDS composites show 95% probability that upper-stratospheric ozone at all latitudes between 60°S and 60°N has increased. This is less robust in
225 SAGE-II/CCI/OMPS and SAGE-II/OSIRIS/OMPS, which show differences at equatorial latitudes (10°S–10°N). The reason for the difference is not clear, but we note that in this region nearly 50% of the data are missing in the first five years (1998–2002), while Merged-SWOOSH/GOZCARDS and Merged-SBUV have no missing data (Harris et al., 2015).

In contrast to the upper stratosphere, all four composites show a consistent ozone decrease below
230 32 hPa / 24 km at all latitudes (Fig. 1). The regions where probabilities are high (>80, 90 and 95%, see legend) are similar in all composites, except for Merged-SBUV which has a lower vertical resolution. Right of Fig. 1a are two examples of the Merged-SBUV vertical resolution, indicating the contribution to ozone at a particular layer, at tropical (solid) and Northern mid-latitudes (dashed)

9

(Kramarova et al., 2013). The profiles peaking at 3 hPa (red) span ~1–8 hPa, and contain only upper
stratospheric changes. However, while changes at 25 hPa (blue) show insignificant changes in the
other higher resolution composites, the Merged-SBUV profile ranges ~15–100 hPa, thus including
the lowest part of the stratosphere where changes in the other composites are negative. We cannot
use Merged-SBUV for comparison of resolved ozone changes, although a total column ozone prod-
uct based upon these data can be used for comparison later (section 4.3). While Merged-SBUV has
a different spatial pattern, the increases in the upper, and decreases in the lower, stratosphere quali-
tatively agree with the other composites. These results strongly indicate that ozone has declined in
the lower stratosphere since 1998.

We note that our spatial results (Figs. 1 and A1) show similar patterns and changes to those pre-
sented in other studies, (e.g.WMO (2014); Bourassa et al. (2014); Sofieva et al. (2017); Steinbrecht
et al. (2017)), though these typically do not extend below 20 km and so often do not show the ex-
tensive decrease in lower stratospheric ozone that we do. Bourassa et al. (2017) extend down to 18
km and, indeed, show a larger region of decreasing ozone trends, but even this does not extend as far
down as our results, i.e. ~17 km for 30°S–30°N, and 13 km outside this region. Our results do not
qualitatively disagree with previous studies and approaches (WMO, 2014). However, four additional
years of data (Tummon et al., 2015; Harris et al., 2015), an improved regression analysis method
(Laine et al., 2014; Ball et al., 2017) (see section 2), and techniques to account for data artefacts
(Ball et al., 2017), **increases our confidence in the identified changes in the lower stratosphere.**

4.2 Stratospheric and Total Column Ozone post-1997 changes

The spatial trends presented in Fig. 1 are informative for understanding where, and assessing why,
changes in stratospheric ozone are occurring. However, stratospheric ozone changes are usually
reported as decadal percentage change vertical profiles or spatial maps (e.g. as in Fig. 1), which
hides the absolute changes in ozone, and the contribution to the total column, which are almost never
reported. A recovery in the upper stratosphere is important to identify, but this region contributes a
smaller fraction to the total column than the middle and lower stratosphere. Thus, smaller percentage
changes over a reduced altitude range in the lower stratosphere can actually produce larger integrated
changes than in the more extended regions higher up.

In Fig. 2 we present changes in partial column ozone in Dobson Units (DU) from Merged-
SWOOSH/GOZCARDS for the whole stratospheric column, and for the upper (10–1 hPa), and
lower stratosphere (147–32 hPa or 13–24 km at >30°; 100–32 hPa or 17–24 km at <30°), respec-
tively. We note that the tropopause, the boundary layer between the troposphere and stratosphere,
varies seasonally, but is on average around 16 km (tropics) and 10–12 km (mid-latitudes); our con-
servative choice of slightly higher altitudes ensures that we avoid including the troposphere. Due to
the near-complete temporal and vertical coverage, we focus on the Merged-SWOOSH/GOZCARDS
composite (SAGE-II/OSIRIS/OMPS and SAGE-II/CCI/OMPS are provided in Figs. A3 and A4,

respectively[5]). Fig. 2 shows posterior distributions of the 1998–2016 ozone changes, with black numbers representing the percentage of the distribution that is negative, in 10° bands (left) and integrated 'global' (defined as 60°S–60°N) partial column ozone (right), along with the total column ozone observed by SBUV (red curves and numbers; upper row).

Upper stratospheric ozone (Fig. 2, middle row) has increased since 1998 in almost all latitude bands, in half the cases at >90% probability, and >95% at 40°–60° in both hemispheres. Globally, the probability exceeds 99% that upper stratospheric ozone has increased, confirming that the MP has indeed been successful in reversing trends in this altitude range.

Changes in the lower stratosphere (Fig. 2, lower row) show ozone decreases, typically exceeding 90% probability (50°S–50°N). There is 99% probability that lower stratospheric ozone has decreased globally (60°S–60°N) since 1998; SAGE-II/OSIRIS/OMPS and SAGE-II/CCI/OMPS both support this result with 87 and 99% probabilities, respectively (Figs. A3 and A4).

Integrating the whole stratosphere vertically, to form the stratospheric column ozone (Fig. 2, upper row), we see that all distributions imply a decrease (i.e. values >50%); probability is generally higher in tropical latitudes (30°S–30°N). Integrating over all latitudes, global stratospheric column ozone (right) indicates that stratospheric ozone has decreased with 95% probability. We compare the Merged-SWOOSH/GOZCARDS change with SBUV total column ozone, the latter of which includes both troposphere and stratosphere. The global SBUV total column ozone indicates that ozone has, in contrast to the stratospheric column ozone, changed little compared to 1998.

We note that uncertainty remains in the middle stratosphere (Fig. A6), with Merged-SWOOSH/GOZCARDS, SAGE-II/CCI/OMPS, and SAGE-II/OSIRIS/OMPS displaying different changes. SAGE-II/OSIRIS/OMPS, in particular, shows a significant positive trend, which leads to the global stratospheric column ozone indicating no change since 1998 (Fig. A3). This is likely a result of how the data were merged to form composites (see examples in Fig A7 at 30 km for northern mid-latitudes and 17 km for southern mid-latitudes, where steps and drifts can be seen in different composites), and is an issue that remains to be resolved (Harris et al., 2015; Ball et al., 2017; Steinbrecht et al., 2017). Nevertheless, the changes in the upper and lower stratosphere are consistent in all ozone composites, and a globally-integrated stratospheric column ozone decline is indicated by both Merged-SWOOSH/GOZCARDS and SAGE-II/CCI/OMPS.

To make these globally-integrated results clear, we show in Fig. 3a the SBUV total column ozone (yellow/red) and Merged-SWOOSH/GOZCARDS stratospheric column ozone (grey/black); in all of the panels in Fig. 3, the timeseries are bias-shifted so that the smoothly varying non-linear trend crosses the zero line in January 1998, so that relative changes can be clearly compared. It is inter-

---

[5]It should be noted that while each latitude band partial column ozone of SAGE-II/OSIRIS/OMPS and SAGE-II/CCI/OMPS typically has between 60 and 90% of months where data are available for 1985–2015/6, integrating bands across all latitudes leads to a reduction of available months (see Fig. A5), though estimates of the change since 1998 can still be made and uncertainties due to the reduced data are captured in the posteriors given in Figs. A3 and A4; this does not affect SBUV total column ozone or Merged-SWOOSH/GOZCARDS.
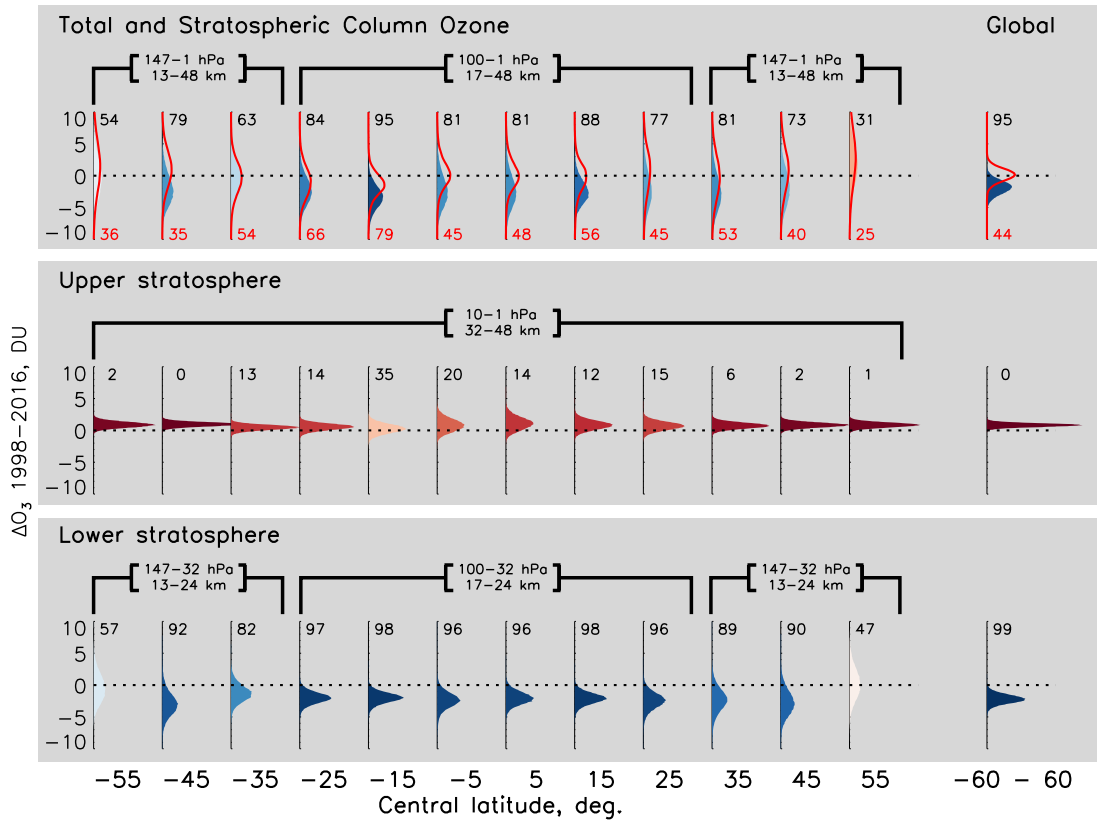
Figure 2: Merged-SWOOSH/GOZCARDS posterior distributions (shaded) for the 1998–2016 total and partial column ozone changes. (Top) whole stratospheric column, (middle) upper and (bottom) lower stratosphere in 10° bands for all latitudes (left) and integrated from 60°S–60°N ('Global', right). The stratosphere extends deeper at mid-latitudes than equatorial (marked above each latitude). Numbers above each distribution represents the distribution-percentage that is negative; colours are graded relative to the percentage-distribution (positive, red-hues, with values <50; negative, blue). SBUV total column ozone (red curves) is given in the upper row and negative distribution-percentages are given as red numbers.

esting to note here that the SBUV total column ozone non-linear trend initially increases from 1998, and then peaks in around 2011, before decreasing. Frith et al. (2014) and Weber et al. (2017) found similar behaviour when applying linear trend fits to SBUV total column ozone, fixing the start date in January 2000 and incrementally increasing the end date, i.e. the largest positive trend was found for the period 2000–2011 and thereafter trends decreased. Their analysis ended in 2013, but the non-linear trend from our DLM analysis, here, shows identical behaviour, and show a continued decrease until 2016, which suggests that total column ozone has now returned to 1998 levels despite an initial upward trend. Qualitatively similar behaviour is seen in the Merged-SWOOSH/GOZCARDS strato-

12

spheric column ozone, though less pronounced because of its larger overall downward behaviour (see below, section 4.3), which lends supporting, independent, evidence that such a turnover in ozone trends might be real. The stratospheric column ozone from Merged-SWOOSH/GOZCARDS continued to decrease after 1998 and, while this decline stalled in the late 2000s, since 2012 it has continued to decrease. The overall result is that stratospheric column ozone is on average lower today than in 1998, by ~1.5 DU.

The different stratospheric regimes that contribute to the stratospheric column ozone behaviour can be see in Figs. 3b–d, where we show, upper, middle (10–32 hPa), and lower stratospheric ozone timeseries from Merged-SWOOSH/GOZCARDS. A recovery is clear in the upper stratosphere in Fig. 3b, increasing by a mean of ~1 DU, and trends have been relatively flat since 1998 in the middle stratosphere (Fig. 3c), with a mean decrease of ~0.5 DU. However, the result from Merged-SWOOSH/GOZCARDS in the lower stratosphere (Fig. 3d) indicates not only that ozone there has declined by ~2 DU since 1998, and has been the main contributor to the stratospheric column ozone decrease, but that the lower stratospheric ozone has seen a *continuous and uninterrupted decrease*. **We note that a large proportion of the post-1997 decline occurred between 2003 and 2006, during which overlaps and switch-overs between different combinations of instrument data were used to form the composites, most notably from the low-sampling SAGE-II instrument that ended operation in 2005; that said, all composites display similar behaviour, and overlaps and switch-overs between different instrument data occur at different times (see Fig. 1 in both Tummon et al. (2015) and Sofieva et al. (2017)).**

4.3 Tropospheric ozone contribution to total column ozone

The stratosphere accounts for the majority (~90%) of total column ozone, so intuitively attribution to total column ozone changes would be expected to come primarily from this region. However, the results in Fig. 2 and 3 suggest a discrepancy between stratospheric column ozone and total column ozone. Despite this, there is no serious conflict between the different changes indicated by global stratospheric column ozone and total column ozone distributions (Fig. 2) and trends (Fig. 3a), when the remaining 10% of the total column ozone, i.e. tropospheric ozone, is considered, as we show in the following.

First, it is important to establish confidence in the SBUV total column ozone observations. These have been very stable since 1998 when comparing SBUV total column ozone overpass data to the independent ground-based Arosa total column ozone observations (Fig. A8). This, therefore, provides confidence in the result that there is little net change in total column ozone since 1998. Additionally, Chehade et al. (2014) reported that other total column ozone composites agree very well with the SBUV total column ozone and there is little difference between the various total column ozone composites when performing trend analysis.

13

In a second step, we consider global tropospheric ozone changes. In Fig. 4, we present recent estimates from OMI/MLS measurements of global (60°S–60°N) tropospheric column ozone from 2004 to 2016 (grey), along with deaseasonalised anomalies (solid black); the deseasonalised years 2005 and 2016 are indicated in blue and red – the means (right) indicate a significant increase in ozone. A linear fit to the deseasonalised timeseries indicates an increase in tropospheric ozone of 1.68 DU per decade; if this has held true for the entire 19 year period (1998–2016) it implies a mean increase of ~3 DU, which would more than account for the difference between the stratospheric column ozone and total column ozone peaks (~1.6 DU) in the upper right panel of Fig. 2.

Supporting evidence for tropospheric ozone increases comes from work reconstructing stratospheric ozone changes in a CCM. Shepherd et al. (2014) indicates that tropospheric ozone in the northern (35°–55°N) and southern mid-latitudes (35°–55°S) may have increased by ~1 DU (1998–2011), while equatorial (25°S–25°N) may have increased by ~1.5 DU respectively. While we consider a longer period, this qualitatively agrees with the latitude-resolved distributions in Fig. 2, which shows that, except for a couple of southern mid-latitudes (30°–40°S and 50°–60°S) and the most northerly band (50°–60°N), all total column ozone posteriors indicate smaller decreases, or larger increases, compared to the Merged-SWOOSH/GOZCARDS stratospheric column ozone changes.

Returning to the OMI/MLS tropospheric column ozone, latitudinally resolved 2005–2015 changes show significant increases everywhere, except a non-significant increase at 50–60S (Fig A13). The latitudinal structure, with peaks at ~30° in both hemispheres and minima at equatorial and high latitudes, bears resemblance to the piecewise linear post-1998 total column ozone trends in Fig. 9 of Chehade et al. (2014) and Fig. 10 of Frith et al. (2014); although more detailed comparisons should be made. OMI/MLS results are not independent from Merged-SWOOSH/GOZCARDS as Aura/MLS forms a part of this composite post-2005, but is independent from SBUV total column ozone. McPeters et al. (2015) states that OMI total column ozone is stable enough for trend studies, with a drift of less than 1% per decade compared to SBUV total column ozone, and is one of the highest quality ozone datasets. Ziemke and Cooper (2017) found no statistically significant drift with respect to independent measures, or between MLS and OMI stratospheric column ozone residuals, although a small drift of +0.5 DU per decade was detected in OMI/MLS tropospheric column ozone caused by an error in the OMI total ozone, which was rectified for the version we consider here.

A deeper investigation is needed to understand the contributions of tropospheric column ozone and stratospheric column ozone to total column ozone, especially considering uncertainties carefully, but this is beyond the scope of this work. We note that studies using various data sources show less significant regional increases (and some decreases) with global estimates ranging from 0.2 to 0.7% per year (~0.6–2 DU per decade) (Cooper et al., 2014; Ebojie et al., 2016; Heue et al., 2016), though these estimates considered different time periods. This suggests a large range of uncertainty, but even the lower end of the estimated increases in tropospheric column ozone are in line with the missing part of the total column ozone change, after considering stratospheric column ozone, that we estimate

14

here. Tropospheric ozone is not the main focus of the study here, but the evidence presented overall suggests the missing component in the declining stratospheric column ozone distributions and trends, with respect to constant total column ozone, is indeed from increasing tropospheric ozone.

4.4 Comparison of stratospheric spatial and partial column ozone trends with models

The observational results for the lower, and whole, stratosphere presented thus far have not been previously reported. However, it is not clear that this represents a departure from our understanding of stratospheric trends as presented in modelling studies. We present the percentage ozone change from two state-of-the-art chemistry climate models (CCMs) in Fig. 5: (a) the NCAR Community Earth System Model (CESM) Whole Atmosphere Community Climate Model-4 (WACCM; Marsh et al. (2013)); and (b) the SOlar Climate Ozone Links (SOCOL; Stenke et al., 2013) model. Both simulations were performed with the Chemistry Climate Model Initiative phase 1 (CCMI-1) boundary conditions in specified dynamics (SD) mode (see Morgenstern et al. (2017) for information on CCMI and boundary conditions used in models). SD uses reanalysis products to constrain model dynamics towards observations so as to best represent the dynamics of the atmosphere, while leaving chemistry to respond freely to these changes. Such an approach has proven highly accurate at reproducing ozone variability on monthly to decadal timescales in the equatorial upper stratosphere (Ball et al., 2016). WACCM-SD uses version 1 of the Modern-Era Retrospective analysis for Research and Applications (MERRA-1; Rienecker et al. (2011) reanalysis[6], while SOCOL-SD uses ERA-Interim (Dee et al., 2011). Thus, the two models are both independent in terms of how they are constructed, and the source of nudging fields used, but have similar boundary conditions as prescribed by CCMI-1.

In Fig. 5 both models display broadly similar behaviour in the upper stratosphere above 10 hPa, roughly in line with the observations (Fig. 1). Spatially, in the middle stratosphere there are differences in sign, but generally significance is low: WACCM-SD displays broadly positive changes except in the tropics at 10 and 30 hPa, while SOCOL-SD displays a negative spot centred in the tropics at 10 hPa, while mid-latitudes are often positive and significant. In the lower stratosphere, SOCOL-SD displays negative trends in the Southern hemisphere lower stratosphere, but positive in the Northern, while WACCM-SD is generally positive everywhere, and significant at the lowest altitudes, except at 30–40 hPa in the tropics where a negative tendency is seen. In both SOCOL-SD and WACCM-SD, trends in the lower stratosphere are generally not significant, and do not display the clear and significant decreases found in the observations. Posterior distributions similar to those of Fig. 2 are presented for SOCOL-SD and WACCM-SD in Figs. A9 and A10, respectively. The displayed behaviour is similar to that described here spatially for the models in Fig. 5, and no sig-

---

[6]Use of MERRA-2 reanalysis (Gelaro et al., 2017) makes little difference, except in the upper stratosphere after 2004, where positive trends are larger when using MERRA-2 (see Fig. A12). The WACCM-SD run with MERRA-2 uses CESM 1.2.2 at 1.9×2.5 horizontal resolution and 88 vertical layers up to 140 km, using prescribed aerosols from the RCP 8.5 scenario.

nificant decreases are found (two SOCOL-SD latitude bands display negative changes in the lower stratosphere with ~75% probability: 30–40S and 10–20N). It is worth noting that in both cases the integrated, global trends in the stratospheric column ozone and upper stratosphere are all positive with probabilities of an increase exceeding 95%, and positive in the lower stratosphere, with 69 and 85% probability of an increase in SOCOL-SD and WACCM-SD, respectively. The non-linear DLM trends (Fig. 3) of WACCM-SD (blue) and SOCOL-SD (purple) emphasize the clearly differing behaviour to the observations, especially in the lower stratosphere (the deaseasonalised and regression model timeseries are omitted from Fig. 3 for clarity, but provided in Fig. A11). It is worth mentioning that the behaviour of total column ozone from the models was similar to SBUV total column ozone (Fig. 3a) until around 2012, after which modelled ozone continued to increase while observations show a gradual decline until 2016 (see discussion in section 4.2).

The CCMVal-2 (SPARC/WMO, 2010) multi-model-mean 2000–2013 ozone changes in the WMO (2014) ozone assessment (Fig. 2-10) show a positive, but insignificant, change in the lower stratosphere at mid-latitudes, which suggests models may not be simulating that region correctly, consistent with the two models extended to 2016 here. While CCMs capture historical ozone behaviour in the upper stratosphere well, it is less clear in the UTLS region. Figs. 7.27–7.28 of the SPARC/WMO (2010) report indicate large differences compared to observations in winter/spring, perhaps related to factors affecting model transport (e.g. resolution, and gravity wave parameterizations). Whether these differences result from model design, incorrect boundary conditions (e.g. underestimated anthropogenic (Yu et al., 2017) or volcanic (Bandoro et al., 2017) aerosol contributions), or missing chemistry, remains an open question.

5 Conclusions

Following the successful implementation of the Montreal Protocol (MP), total column ozone stabilised at the end of the 1990s, and searches for the first signs of recovery in total column ozone have been underway since then (Weber et al., 2017; Chipperfield et al., 2017). We find that counteracting trends within different atmospheric layers are the reason a significant detection has remained elusive. In summary, we have presented evidence of highly significant changes in stratospheric ozone between 1998 and 2016. The main findings are that:

(i) the MP is further confirmed to be successfully reducing the impact of hODSs as indicated by the highly probable recovery seen in most upper stratospheric (1–10 hPa / 32–48 km) regions in all composites;

(ii) lower stratospheric ozone (147/100–32 hPa / 13/17–24 km) has continued to decrease since 1998 at all latitudes between 50°S and 50°N;

16

(iii) there are indications that the total, global (60°S–60°N) stratospheric ozone may have continued
450   to decrease;

(iv) indications of no decrease, or perhaps an increase, in total column ozone is likely a result of
increasing tropospheric ozone, together with the slowed rate of decrease in stratospheric ozone
following the MP.

(v) state-of-the-art models, nudged to have historical atmospheric dynamics as realistic as possible
455   do not reproduce the observed decreases in lower stratospheric ozone, which may suggest
deficiencies in some aspect of the modelling.

We posit several possible explanations for the continuing decline in lower stratospheric ozone. Part of the tropical (<30°) lower stratospheric decline may be linked to a greenhouse gas (GHG)-related BDC acceleration (Randel and Wu, 2007; Oman et al., 2010; WMO, 2014), in-
460 **dicated from CCM simulations, although observational evidence remains weak (WMO, 2014). A rise in the tropopause (Santer et al., 2003), due to the warming troposphere, could lead to a localised ozone decrease (Steinbrecht et al., 1998), though large-scale impacts on total column ozone are unclear (Plummer et al., 2010; Dietmüller et al., 2014). We hypothesize an acceleration of the lower stratosphere BDC shallow branch (Randel and Wu, 2007; Oman et al., 2010)**
465 **might increase transport of ozone-poor air to the mid-latitudes from the tropical lower stratosphere (Johnston, 1975; Perliski et al., 1989). While dynamically driven explanations may be more likely for tropical lower stratospheric ozone changes, a chemically-driven contributor at mid-latitudes may additionally come from increasing anthropogenic and natural very short lived substances (VSLSs) containing chlorine and bromine species (Hossaini et al., 2015). Mod-**
470 **elling studies imply that VSLSs preferentially destroy lower stratospheric ozone, though the effect outside of the polar latitudes is expected to be quite small (Hossaini et al., 2015, 2017). While VSLSs are only thought to delay the recovery of the ozone layer, much uncertainty remains since observations and reaction rate kinetics are only available for some VSLSs (Oram et al., 2017).**

475 **The MP is working, but if the lower stratospheric trends continue there are likely consequences. Less significant is reduced stratosphere-troposphere ozone exchange, (Hegglin and Shepherd, 2009; Neu et al., 2014), and a small, additional offset of GHG radiative forcing (RF) leading to a minor reduction in the warming of the climate (Randel and Thompson, 2011). Most significantly, restoration of the ozone layer is essential to reducing the harmful effects of**
480 **solar UV radiation that impact surface life, and human and ecosystem health (Slaper et al., 1996); returning surface UV radiation to pre-1980's levels depends on the total column ozone (WMO, 2014). Models do not yet reproduce the downward trend with significance. So it is imperative that we determine the cause of the decline in lower stratospheric ozone identified here, both to predict future changes, and to determine if it is possible to prevent further decreases.**

17

References

Ball, W. T., Haigh, J. D., Rozanov, E. V., Kuchar, A., Sukhodolov, T., Tummon, F., Shapiro, A. V., and Schmutz,
495   W.: High solar cycle spectral variations inconsistent with stratospheric ozone observations, Nature Geo-
science, 9, 206–209, doi:10.1038/ngeo2640, 2016.

Ball, W. T., Alsing, J., Mortlock, D. J., Rozanov, E. V., Tummon, F., and Haigh, J. D.: Reconciling differences
in stratospheric ozone composites, Atmospheric Chemistry & Physics, 17, 12 269–12 302, doi:10.5194/acp-
17-12269-2017, 2017.

500   Bandoro, J., Solomon, S., Santer, B. D., Kinnison, D. E., and Mills, M. J.: Detectability of the Impacts of Ozone
Depleting Substances and Greenhouse Gases upon Stratospheric Ozone Accounting for Nonlinearities in
Historical Forcings, Atmospheric Chemistry and Physics Discussions, 2017, 1–42, doi:10.5194/acp-2017-
585, https://www.atmos-chem-phys-discuss.net/acp-2017-585/, 2017.

Bourassa, A. E., Degenstein, D. A., Randel, W. J., Zawodny, J. M., Kyrölä, E., McLinden, C. A., Sioris, C. E.,
505   and Roth, C. Z.: Trends in stratospheric ozone derived from merged SAGE II and Odin-OSIRIS satellite
observations, Atmos. Chem. Phys., 14, 6983–6994, doi:10.5194/acp-14-6983-2014, 2014.

Bourassa, A. E., Roth, C. Z., Zawada, D. J., Rieger, L. A., McLinden, C. A., and Degenstein, D. A.: Drift
corrected Odin-OSIRIS ozone product: algorithm and updated stratospheric ozone trends, Atmos. Meas.
Tech. Discuss., doi:10.5194/amt-2017-229, 2017.

510   Chehade, W., Weber, M., and Burrows, J. P.: Total ozone trends and variability during 1979-2012 from merged
data sets of various satellites, Atmospheric Chemistry & Physics, 14, 7059–7074, doi:10.5194/acp-14-7059-
2014, 2014.

Chiodo, G., Marsh, D. R., Garcia-Herrera, R., Calvo, N., and García, J. A.: On the detection of the solar signal
in the tropical stratosphere, Atmospheric Chemistry & Physics, 14, 5251–5269, doi:10.5194/acp-14-5251-
515   2014, 2014.

Chipperfield, M. P., Bekki, S., Dhomse, S., Harris, N. R. P., Hassler, B., Hossaini, R., Steinbrecht, W., Thiéble-
mont, R., and Weber, M.: Detecting recovery of the stratospheric ozone layer, Nature, 549, 211–218,
doi:10.1038/nature23681, 2017.

Cooper, O. R., Parrish, D. D., Ziemke, J., Balashov, N. V., Cupeiro, M., Galbally, I. E., Gilge, S., Horowitz,
520   L., Jensen, N. R., Lamarque, J.-F., Naik, V., Oltmans, S. J., J., S., T., S. D., Thompson, A. M., Thouret, V.,
Wang, Y., and Zbinden, R. M.: Global distribution and trends of tropospheric ozone: An observation-based
review, Elem Sci Anth., p. 29, doi:10.12952/journal.elementa.000029, 2014.

Damadeo, R. P., Zawodny, J. M., and Thomason, L. W.: Reevaluation of stratospheric ozone trends from SAGE
II data using a simultaneous temporal and spatial analysis, Atmospheric Chemistry & Physics, 14, 13 455–
525   13 470, doi:10.5194/acp-14-13455-2014, 2014.

Davis, S. M., Rosenlof, K. H., Hassler, B., Hurst, D. F., Read, W. G., Vömel, H., Selkirk, H., Fujiwara, M., and
Damadeo, R.: The Stratospheric Water and Ozone Satellite Homogenized (SWOOSH) database: a long-term
database for climate studies, Earth System Science Data, 8, 461–490, doi:10.5194/essd-8-461-2016, 2016.

Dee, D. P., Uppala, S. M., Simmons, A. J., Berrisford, P., Poli, P., Kobayashi, S., Andrae, U., Balmaseda,
530   M. A., Balsamo, G., Bauer, P., Bechtold, P., Beljaars, A. C. M., van de Berg, L., Bidlot, J., Bormann, N.,
Delsol, C., Dragani, R., Fuentes, M., Geer, A. J., Haimberger, L., Healy, S. B., Hersbach, H., Hólm, E. V.,
Isaksen, L., Kållberg, P., Köhler, M., Matricardi, M., McNally, A. P., Monge-Sanz, B. M., Morcrette, J.-

J., Park, B.-K., Peubey, C., de Rosnay, P., Tavolato, C., Thépaut, J.-N., and Vitart, F.: The ERA-Interim reanalysis: configuration and performance of the data assimilation system, Quarterly Journal of the Royal Meteorological Society, 137, 553–597, doi:10.1002/qj.828, 2011.

Dietmüller, S., Ponater, M., and Sausen, R.: Interactive ozone induces a negative feedback in CO_2-driven climate change simulations, Journal of Geophysical Research (Atmospheres), 119, 1796–1805, doi:10.1002/2013JD020575, 2014.

Dudok de Wit, T., Bruinsma, S., and Shibasaki, K.: Synoptic radio observations as proxies for upper atmosphere modelling, Journal of Space Weather and Space Climate, 4, A06, doi:10.1051/swsc/2014003, 2014.

Ebojie, F., Burrows, J. P., Gebhardt, C., Ladstätter-Weißenmayer, A., von Savigny, C., Rozanov, A., Weber, M., and Bovensmann, H.: Global tropospheric ozone variations from 2003 to 2011 as seen by SCIAMACHY, Atmospheric Chemistry & Physics, 16, 417–436, doi:10.5194/acp-16-417-2016, 2016.

Eyring, V., Cionni, I., Bodeker, G. E., Charlton-Perez, A. J., Kinnison, D. E., Scinocca, J. F., Waugh, D. W., Akiyoshi, H., Bekki, S., Chipperfield, M. P., Dameris, M., Dhomse, S., Frith, S. M., Garny, H., Gettelman, A., Kubin, A., Langematz, U., Mancini, E., Marchand, M., Nakamura, T., Oman, L. D., Pawson, S., Pitari, G., Plummer, D. A., Rozanov, E., Shepherd, T. G., Shibata, K., Tian, W., Braesicke, P., Hardiman, S. C., Lamarque, J. F., Morgenstern, O., Pyle, J. A., Smale, D., and Yamashita, Y.: Multi-model assessment of stratospheric ozone return dates and ozone recovery in CCMVal-2 models, Atmospheric Chemistry & Physics, 10, 9451–9472, doi:10.5194/acp-10-9451-2010, 2010.

Farman, J. C., Gardiner, B. G., and Shanklin, J. D.: Large losses of total ozone in Antarctica reveal seasonal ClO_x/NO_x interaction, Nature, 315, 207–210, doi:10.1038/315207a0, 1985.

Frith, S. M., Kramarova, N. A., Stolarski, R. S., McPeters, R. D., Bhartia, P. K., and Labow, G. J.: Recent changes in total column ozone based on the SBUV Version 8.6 Merged Ozone Data Set, Journal of Geophysical Research (Atmospheres), 119, 9735–9751, doi:10.1002/2014JD021889, 2014.

Frith, S. M., Stolarski, R. S., Kramarova, N. A., and McPeters: Estimating Uncertainties in the SBUV Version 8.6 Merged Profile Ozone Dataset, Atmos. Phys. Chem. Disc., doi:10.5194/acp-2017-412, 2017.

Froidevaux, L., Anderson, J., Wang, H.-J., Fuller, R. A., Schwartz, M. J., Santee, M. L., Livesey, N. J., Pumphrey, H. C., Bernath, P. F., Russell, III, J. M., and McCormick, M. P.: Global OZone Chemistry And Related trace gas Data records for the Stratosphere (GOZCARDS): methodology and sample results with a focus on HCl, H_2O, and O_3, Atmospheric Chemistry & Physics, 15, 10 471–10 507, doi:10.5194/acp-15-10471-2015, 2015.

Gebhardt, C., Rozanov, A., Hommel, R., Weber, M., Bovensmann, H., Burrows, J. P., Degenstein, D., Froidevaux, L., and Thompson, A. M.: Stratospheric ozone trends and variability as seen by SCIAMACHY from 2002 to 2012, Atmospheric Chemistry & Physics, 14, 831–846, doi:10.5194/acp-14-831-2014, 2014.

Gelaro, R., McCarty, W., Suárez, M. J., Todling, R., Molod, A., Takacs, L., Randles, C. A., Darmenov, A., Bosilovich, M. G., Reichle, R., Wargan, K., Coy, L., Cullather, R., Draper, C., Akella, S., Buchard, V., Conaty, A., da Silva, A. M., Gu, W., Kim, G.-K., Koster, R., Lucchesi, R., Merkova, D., Nielsen, J. E., Partyka, G., Pawson, S., Putman, W., Rienecker, M., Schubert, S. D., Sienkiewicz, M., and Zhao, B.: The Modern-Era Retrospective Analysis for Research and Applications, Version 2 (MERRA-2), Journal of Climate, 30, 5419–5454, doi:10.1175/JCLI-D-16-0758.1, 2017.

Harris, N. R. P., Hassler, B., Tummon, F., Bodeker, G. E., Hubert, D., Petropavlovskikh, I., Steinbrecht, W., Anderson, J., Bhartia, P. K., Boone, C. D., Bourassa, A., Davis, S. M., Degenstein, D., Delcloo, A., Frith, S. M., Froidevaux, L., Godin-Beekmann, S., Jones, N., Kurylo, M. J., Kyrölä, E., Laine, M., Leblanc, S. T., Lambert, J.-C., Liley, B., Mahieu, E., Maycock, A., de Mazière, M., Parrish, A., Querel, R., Rosenlof, K. H., Roth, C., Sioris, C., Staehelin, J., Stolarski, R. S., Stübi, R., Tamminen, J., Vigouroux, C., Walker, K. A., Wang, H. J., Wild, J., and Zawodny, J. M.: Past changes in the vertical distribution of ozone - Part 3: Analysis and interpretation of trends, Atmospheric Chemistry & Physics, 15, 9965–9982, doi:10.5194/acp-15-9965-2015, 2015.

Hegglin, M. I. and Shepherd, T. G.: Large climate-induced changes in ultraviolet index and stratosphere-to-troposphere ozone flux, Nature Geoscience, 2, 687–691, doi:10.1038/ngeo604, 2009.

Heue, K.-P., Coldewey-Egbers, M., Delcloo, A., Lerot, C., Loyola, D., Valks, P., and van Roozendael, M.: Trends of tropical tropospheric ozone from 20 years of European satellite measurements and perspectives for the Sentinel-5 Precursor, Atmospheric Measurement Techniques, 9, 5037–5051, doi:10.5194/amt-9-5037-2016, 2016.

Hossaini, R., Chipperfield, M. P., Montzka, S. A., Rap, A., Dhomse, S., and Feng, W.: Efficiency of short-lived halogens at influencing climate through depletion of stratospheric ozone, Nature Geoscience, 8, 186–190, doi:10.1038/ngeo2363, 2015.

Hossaini, R., Chipperfield, M. P., Montzka, S. A., Leeson, A. A., Dhomse, S., and Pyle, J. A.: The increasing threat to stratospheric ozone from dichloromethane, Nature Communications, 8, doi:10.1038/ncomms15962, 2017.

Johnston, H. S.: Global ozone balance in the natural stratosphere, Reviews of Geophysics and Space Physics, 13, 637–649, doi:10.1029/RG013i005p00637, 1975.

Kramarova, N. A., Bhartia, P. K., Frith, S. M., McPeters, R. D., and Stolarski, R. S.: Interpreting SBUV smoothing errors: an example using the quasi-biennial oscillation, Atmospheric Measurement Techniques, 6, 2089–2099, doi:10.5194/amt-6-2089-2013, 2013.

Kyrölä, E., Laine, M., Sofieva, V., Tamminen, J., Päivärinta, S.-M., Tukiainen, S., Zawodny, J., and Thomason, L.: Combined SAGE II-GOMOS ozone profile data set for 1984-2011 and trend analysis of the vertical distribution of ozone, Atmospheric Chemistry & Physics, 13, 10 645–10 658, doi:10.5194/acp-13-10645-2013, 2013.

Laine, M., Latva-Pukkila, N., and Kyrölä, E.: Analysing time-varying trends in stratospheric ozone time series using the state space approach, Atmospheric Chemistry & Physics, 14, 9707–9725, doi:10.5194/acp-14-9707-2014, 2014.

Marsh, D. R. and Garcia, R. R.: Attribution of decadal variability in lower-stratospheric tropical ozone, Geophysical Research Letters, 34, L21807, doi:10.1029/2007GL030935, 2007.

Marsh, D. R., Mills, M. J., Kinnison, D. E., Lamarque, J.-F., Calvo, N., and Polvani, L. M.: Climate Change from 1850 to 2005 Simulated in CESM1(WACCM), Journal of Climate, 26, 7372–7391, doi:10.1175/JCLI-D-12-00558.1, 2013.

McPeters, R. D., Bhartia, P. K., Haffner, D., Labow, G. J., and Flynn, L.: The version 8.6 SBUV ozone data record: An overview, Journal of Geophysical Research (Atmospheres), 118, 8032–8039, doi:10.1002/jgrd.50597, 2013.

McPeters, R. D., Frith, S., and Labow, G. J.: OMI total column ozone: extending the long-term data record, Atmospheric Measurement Techniques, 8, 4845–4850, doi:10.5194/amt-8-4845-2015, 2015.

Molina, M. J. and Rowland, F. S.: Stratospheric sink for chlorofluoromethanes: chlorine atomc-atalysed destruction of ozone, Nature, 249, 810–812, doi:10.1038/249810a0, 1974.

Morgenstern, O., Hegglin, M. I., Rozanov, E., O'Connor, F. M., Abraham, N. L., Akiyoshi, H., Archibald, A. T., Bekki, S., Butchart, N., Chipperfield, M. P., Deushi, M., Dhomse, S. S., Garcia, R. R., Hardiman, S. C., Horowitz, L. W., Jöckel, P., Josse, B., Kinnison, D., Lin, M., Mancini, E., Manyin, M. E., Marchand, M., Marécal, V., Michou, M., Oman, L. D., Pitari, G., Plummer, D. A., Revell, L. E., Saint-Martin, D., Schofield, R., Stenke, A., Stone, K., Sudo, K., Tanaka, T. Y., Tilmes, S., Yamashita, Y., Yoshida, K., and Zeng, G.: Review of the global models used within phase 1 of the Chemistry-Climate Model Initiative (CCMI), Geoscientific Model Development, 10, 639–671, doi:10.5194/gmd-10-639-2017, 2017.

Nair, P. J., Froidevaux, L., Kuttippurath, J., Zawodny, J. M., Russell, J. M., Steinbrecht, W., Claude, H., Leblanc, T., van Gijsel, J. A. E., Johnson, B., Swart, D. P. J., Thomas, A., Querel, R., Wang, R., and Anderson, J.: Subtropical and midlatitude ozone trends in the stratosphere: Implications for recovery, Journal of Geophysical Research (Atmospheres), 120, 7247–7257, doi:10.1002/2014JD022371, 2015.

NCAR: The Climate Data Guide: Multivariate ENSO Index, Retrieved from https://climatedataguide.ucar.edu/climate-data/multivariate-enso-index, 2013.

Neu, J. L., Flury, T., Manney, G. L., Santee, M. L., Livesey, N. J., and Worden, J.: Tropospheric ozone variations governed by changes in stratospheric circulation, Nature Geoscience, 7, 340–344, doi:10.1038/ngeo2138, 2014.

Newman, P. A., Daniel, J. S., Waugh, D. W., and Nash, E. R.: A new formulation of equivalent effective stratospheric chlorine (EESC), Atmospheric Chemistry & Physics, 7, 4537–4552, 2007.

Nowack, P. J., Luke Abraham, N., Maycock, A. C., Braesicke, P., Gregory, J. M., Joshi, M. M., Osprey, A., and Pyle, J. A.: A large ozone-circulation feedback and its implications for global warming assessments, Nature Climate Change, 5, 41–45, doi:10.1038/nclimate2451, 2015.

Oman, L. D., Plummer, D. A., Waugh, D. W., Austin, J., Scinocca, J. F., Douglass, A. R., Salawitch, R. J., Canty, T., Akiyoshi, H., Bekki, S., Braesicke, P., Butchart, N., Chipperfield, M. P., Cugnet, D., Dhomse, S., Eyring, V., Frith, S., Hardiman, S. C., Kinnison, D. E., Lamarque, J.-F., Mancini, E., Marchand, M., Michou, M., Morgenstern, O., Nakamura, T., Nielsen, J. E., Olivié, D., Pitari, G., Pyle, J., Rozanov, E., Shepherd, T. G., Shibata, K., Stolarski, R. S., TeyssèDre, H., Tian, W., Yamashita, Y., and Ziemke, J. R.: Multimodel assessment of the factors driving stratospheric ozone evolution over the 21st century, Journal of Geophysical Research (Atmospheres), 115, D24306, doi:10.1029/2010JD014362, 2010.

Oram, D. E., Ashfold, M. J., Laube, J. C., Gooch, L. J., Humphrey, S., Sturges, W. T., Leedham-Elvidge, E., Forster, G. L., Harris, N. R. P., Mead, M. I., Abu Samah, A., Moi Phang, S., Ou-Yang, C.-F., Lin, N.-H., Wang, J.-L., Baker, A. K., Brenninkmeijer, C. A. M., and Sherry, D.: A growing threat to the ozone layer from short-lived anthropogenic chlorocarbons, Atmospheric Chemistry & Physics, 17, 11 929–11 941, doi:10.5194/acp-17-11929-2017, 2017.

Perliski, L. M., London, J., and Solomon, S.: On the interpretation of seasonal variations of stratospheric ozone, Journal of Geophysical Research, 37, 1527–1538, doi:10.1016/0032-0633(89)90143-8, 1989.

22

Plummer, D. A., Scinocca, J. F., Shepherd, T. G., Reader, M. C., and Jonsson, A. I.: Quantifying the contributions to stratospheric ozone changes from ozone depleting substances and greenhouse gases, Atmospheric Chemistry & Physics, 10, 8803–8820, doi:10.5194/acp-10-8803-2010, 2010.

Randel, W. J. and Thompson, A. M.: Interannual variability and trends in tropical ozone derived from SAGE II satellite data and SHADOZ ozonesondes, Journal of Geophysical Research (Atmospheres), 116, D07303, doi:10.1029/2010JD015195, 2011.

Randel, W. J. and Wu, F.: A stratospheric ozone profile data set for 1979-2005: Variability, trends, and comparisons with column ozone data, Journal of Geophysical Research (Atmospheres), 112, D06313, doi:10.1029/2006JD007339, 2007.

Revell, L. E., Bodeker, G. E., Huck, P. E., Williamson, B. E., and Rozanov, E.: The sensitivity of stratospheric ozone changes through the 21st century to N_2O and CH_4, Atmospheric Chemistry & Physics, 12, 11 309–11 317, doi:10.5194/acp-12-11309-2012, 2012.

Rienecker, M. M., Suarez, M. J., Gelaro, R., Todling, R., Bacmeister, J., Liu, E., Bosilovich, M. G., Schubert, S. D., Takacs, L., Kim, G.-K., Bloom, S., Chen, J., Collins, D., Conaty, A., da Silva, A., Gu, W., Joiner, J., Koster, R. D., Lucchesi, R., Molod, A., Owens, T., Pawson, S., Pegion, P., Redder, C. R., Reichle, R., Robertson, F. R., Ruddick, A. G., Sienkiewicz, M., and Woollen, J.: MERRA: NASA's Modern-Era Retrospective Analysis for Research and Applications, Journal of Climate, 24, 3624–3648, doi:10.1175/JCLI-D-11-00015.1, 2011.

Santer, B. D., Wehner, M. F., Wigley, T. M. L., Sausen, R., Meehl, G. A., Taylor, K. E., Ammann, C., Arblaster, J., Washington, W. M., Boyle, J. S., and Brüggemann, W.: Contributions of Anthropogenic and Natural Forcing to Recent Tropopause Height Changes, Science, 301, 479–483, doi:10.1126/science.1084123, 2003.

Scarnato, B., Staehelin, J., Stübi, R., and Schill, H.: Long-term total ozone observations at Arosa (Switzerland) with Dobson and Brewer instruments (1988-2007), Journal of Geophysical Research (Atmospheres), 115, D13306, doi:10.1029/2009JD011908, 2010.

Shepherd, T. G., Plummer, D. A., Scinocca, J. F., Hegglin, M. I., Fioletov, V. E., Reader, M. C., Remsberg, E., von Clarmann, T., and Wang, H. J.: Reconciliation of halogen-induced ozone loss with the total-column ozone record, Nature Geoscience, 7, 443–449, doi:10.1038/ngeo2155, 2014.

Sioris, C. E., McLinden, C. A., Fioletov, V. E., Adams, C., Zawodny, J. M., Bourassa, A. E., Roth, C. Z., and Degenstein, D. A.: Trend and variability in ozone in the tropical lower stratosphere over 2.5 solar cycles observed by SAGE II and OSIRIS, Atmospheric Chemistry & Physics, 14, 3479–3496, doi:10.5194/acp-14-3479-2014, 2014.

Slaper, H., Velders, G. J. M., Daniel, J. S., de Gruijl, F. R., and van der Leun, J. C.: Estimates of ozone depletion and skin cancer incidence to examine the Vienna Convention achievements, Nature, 384, 256–258, doi:10.1038/384256a0, 1996.

Sofieva, V., Kyrölä, E., Laine, M., Tamminen, J., Degenstein, D., Bourassa, A., Roth, C., Zawada, D., Weber, M., Rozanov, A., Rahpoe, N., Stiller, G., Laeng, A., von Clarmann, T., Walker, K., Sheese, P., Hubert, D., van Roozendael, M., Zehner, C., Damadeo, R., Zawodny, J., Kramarova, N., , and Bhartia, P.: Merged SAGE II, Ozone_cci and OMPS ozone profiles dataset and evaluation of ozone trends in the stratosphere, Atmos. Chem. Phys. Discuss., doi:10.5194/acp-2017-598, 2017.

23

690 Sofieva, V. F., Kalakoski, N., Päivärinta, S.-M., Tamminen, J., Laine, M., and Froidevaux, L.: On sampling uncertainty of satellite ozone profile measurements, Atmospheric Measurement Techniques, 7, 1891–1900, doi:10.5194/amt-7-1891-2014, 2014.

Solomon, S., Ivy, D. J., Kinnison, D., Mills, M. J., Neely, R. R., and Schmidt, A.: Emergence of healing in the Antarctic ozone layer, Science, 353, 269–274, doi:10.1126/science.aae0061, 2016.

695 SPARC/WMO: SPARC Report on the Evaluation of Chemistry-Climate Models, SPARC, 2010.

Steinbrecht, W., Claude, H., KöHler, U., and Hoinka, K. P.: Correlations between tropopause height and total ozone: Implications for long-term changes, Journal of Geophysical Research, 103, 19, doi:10.1029/98JD01929, 1998.

Steinbrecht, W., Froidevaux, L., Fuller, R., Wang, R., Anderson, J., Roth, C., Bourassa, A., Degenstein, D.,
700 Damadeo, R., Zawodny, J., Frith, S., McPeters, R., Bhartia, P., Wild, J., Long, C., Davis, S., Rosenlof, K., Sofieva, V., Walker, K., Rahpoe, N., Rozanov, A., Weber, M., Laeng, A., von Clarmann, T., Stiller, G., Kramarova, N., Godin-Beekmann, S., Leblanc, T., Querel, R., Swart, D., Boyd, I., Hocke, K., Kämpfer, N., Maillard Barras, E., Moreira, L., Nedoluha, G., Vigouroux, C., Blumenstock, T., Schneider, M., Garcìa, O., Jones, N., Mahieu, E., Smale, D., Kotkamp, M., Robinson, J., Petropavlovskikh, I., Harris, N., Hassler,
705 B., Hubert, D., and Tummon, F.: An update on ozone profile trends for the period 2000 to 2016, Atmos. Chem. Phys. Discuss., 2017, 1–24, doi:10.5194/acp-2017-391, https://www.atmos-chem-phys-discuss.net/ acp-2017-391/, 2017.

Stenke, A., Schraner, M., Rozanov, E., Egorova, T., Luo, B., and Peter, T.: The SOCOL version 3.0 chemistry-climate model: description, evaluation, and implications from an advanced transport algorithm, Geoscientific
710 Model Development, 6, 1407–1427, doi:10.5194/gmd-6-1407-2013, 2013.

Tegtmeier, S., Hegglin, M. I., Anderson, J., Bourassa, A., Brohede, S., Degenstein, D., Froidevaux, L., Fuller, R., Funke, B., Gille, J., Jones, A., Kasai, Y., Krüger, K., Kyrölä, E., Lingenfelser, G., Lumpe, J., Nardi, B., Neu, J., Pendlebury, D., Remsberg, E., Rozanov, A., Smith, L., Toohey, M., Urban, J., Clarmann, T., Walker, K. A., and Wang, R. H. J.: SPARC Data Initiative: A comparison of ozone climatolo-
715 gies from international satellite limb sounders, Journal of Geophysical Research (Atmospheres), 118, 12, doi:10.1002/2013JD019877, 2013.

Thomason, L., Ernest, N., Millan, L., Rieger, L., Bourassa, A., Vernier, J., Peter, T., Luo, B., and Arfeuille, F.: A global, space-based stratospheric aerosol climatology: 1979 to 2016, Earth Syst. Sci. Data, in preparation, doi:10.5067/GloSSAC-L3-V1.0, 2017.

720 Tiao, G. C., Xu, D., Pedrick, J. H., Zhu, X., and Reinsel, G. C.: Effects of autocorrelation and temporal sampling schemes on estimates of trend and spatial correlation, Journal of Geophysical Research, 95, 20 507–20 517, doi:10.1029/JD095iD12p20507, 1990.

Tummon, F., Hassler, B., Harris, N. R. P., Staehelin, J., Steinbrecht, W., Anderson, J., Bodeker, G. E., Bourassa, A., Davis, S. M., Degenstein, D., Frith, S. M., Froidevaux, L., Kyrölä, E., Laine, M., Long, C., Penckwitt,
725 A. A., Sioris, C. E., Rosenlof, K. H., Roth, C., Wang, H.-J., and Wild, J.: Intercomparison of vertically resolved merged satellite ozone data sets: interannual variability and long-term trends, Atmospheric Chemistry & Physics, 15, 3021–3043, doi:10.5194/acp-15-3021-2015, 2015.

Vigouroux, C., Blumenstock, T., Coffey, M., Errera, Q., García, O., Jones, N. B., Hannigan, J. W., Hase, F., Liley, B., Mahieu, E., Mellqvist, J., Notholt, J., Palm, M., Persson, G., Schneider, M., Servais, C., Smale,

24

730   D., Thölix, L., and De Mazière, M.: Trends of ozone total columns and vertical distribution from FTIR observations at eight NDACC stations around the globe, Atmospheric Chemistry & Physics, 15, 2915–2933, doi:10.5194/acp-15-2915-2015, 2015.

Weber, M., Coldewey-Egbers, M., Fioletov, V. E., Frith, S. M., Wild, J. D., Burrows, J. P., Long, C. S., and Loyola, D.: Total ozone trends from 1979 to 2016 derived from five merged observational datasets - the

735   emergence into ozone recovery, Atmos. Chem. Phys. Discuss., 2017.

Wild, J. D. and Long, C. S.: A Coherent Ozone Profile Dataset from SBUV, SBUV/2: 1979 to 2016, in preparation, 2017.

WMO: Scientific Assessment of Ozone Depletion: 2006, Global Ozone Research and Monitoring Project, 2006.

WMO: Scientific Assessment of Ozone Depletion: 2010, Global Ozone Research and Monitoring Project, 52,

740   516, 2011.

WMO: Scientific Assessment of Ozone Depletion: 2014 Global Ozone Research and Monitoring Project Report, World Meteorological Organization, p. 416, geneva, Switzerland, 2014.

WMO/NASA: International Ozone Trends Panel Report, Report, 1988.

Yu, P., Rosenlof, K. H., Liu, S., Telg, H., Thornberry, T. D., Rollins, A. W., Portmann, R. W., Bai, Z., Ray,

745   E. A., Duan, Y., Pan, L. L., Toon, O. B., Bian, J., and Gao, R.-S.: Efficient transport of tropospheric aerosol into the stratosphere via the Asian summer monsoon anticyclone, Proceedings of the National Academy of Science, 114, 6972–6977, doi:10.1073/pnas.1701170114, 2017.

Ziemke, J. R. and Cooper, O. R.: Tropospheric ozone, in State of the Climate in 2016, Bull. Amer. Meteorol., in press, 2017.

750   Ziemke, J. R., Chandra, S., Duncan, B. N., Froidevaux, L., Bhartia, P. K., Levelt, P. F., and Waters, J. W.: Tropospheric ozone determined from Aura OMI and MLS: Evaluation of measurements and comparison with the Global Modeling Initiative's Chemical Transport Model, Journal of Geophysical Research (Atmospheres), 111, D19303, doi:10.1029/2006JD007089, 2006.
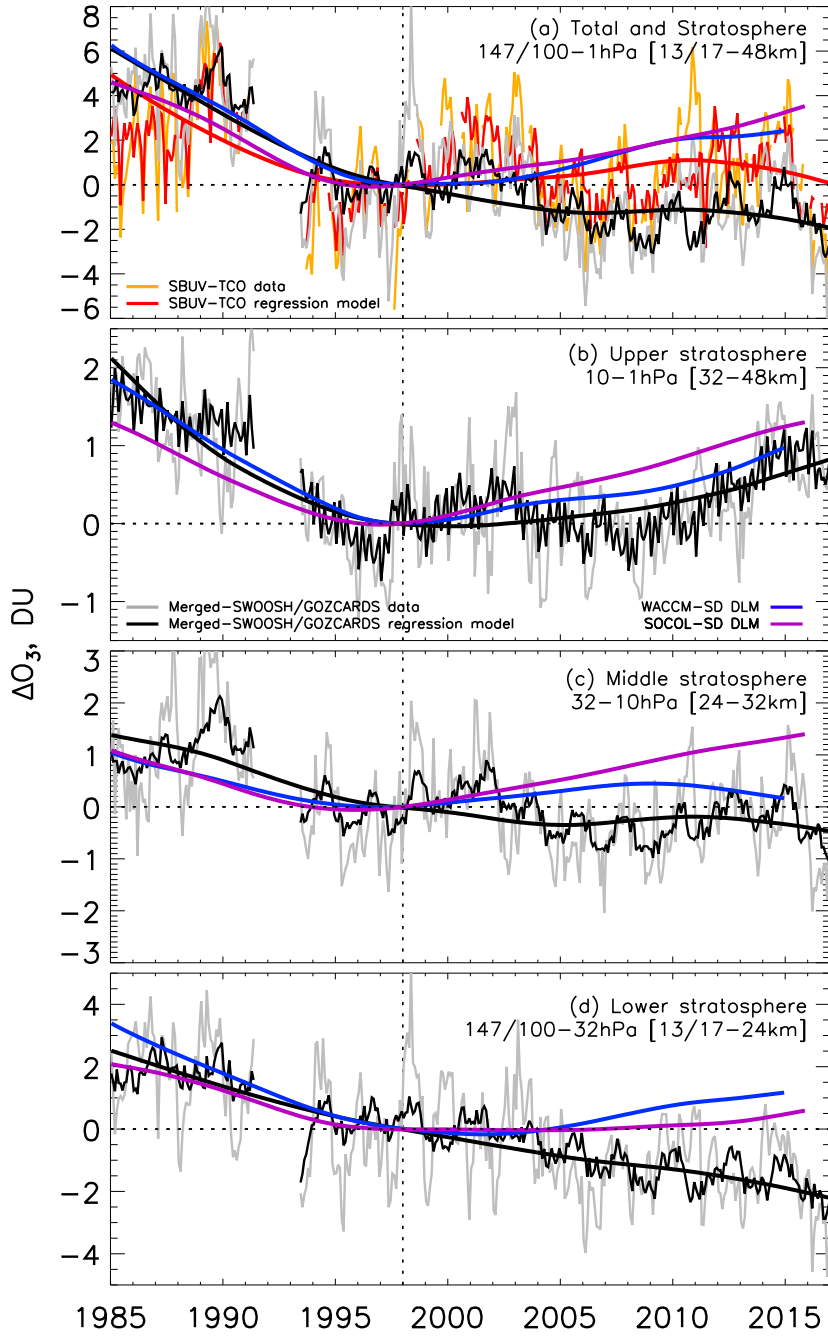
Figure 3: 'Global' 60°S–60°N 1985–2016 total and partial column ozone anomalies. Deseasonalised and regression model timeseries are given for the Merged-SWOOSH/GOZCARDS merged composite (grey and black, respectively) for (a) the whole stratospheric column, (b) upper, (c) middle, and (d) lower stratospheric partial column ozone. The DLM non-linear trend is the smoothly varying thick black line. In (a), the deseasonalised SBUV total column ozone is also given (orange), with the regression model (red) and the non-linear trend (thick, red). Data are shifted so the trend-line is zero in 1998. DLM results for WACCM-SD (blue) and SOCOL-SD (purple) from Fig. A11 are also shown.
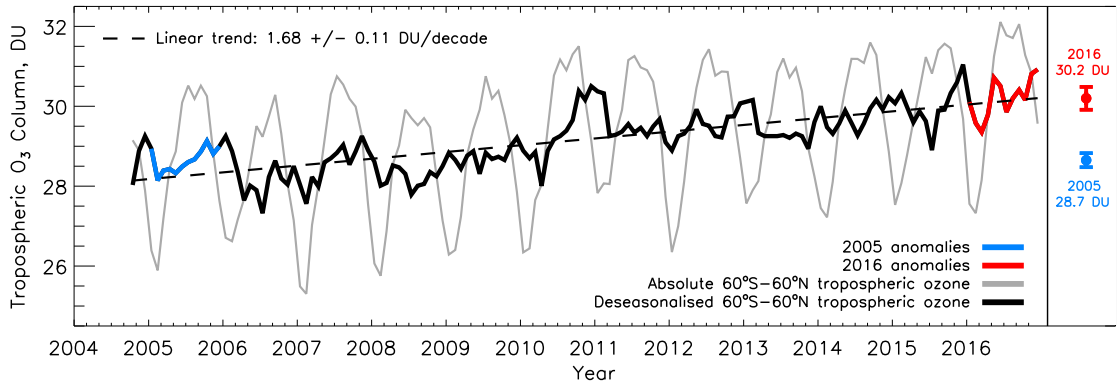
Figure 4: 'Global' 60°S–60°N total tropospheric column ozone between 2004 and 2016. OMI/MLS integrated ozone (grey line) and deseasonalised timeseries (black). The 2005 and 2016 periods are plotted in blue and red, respectively and the mean and two standard errors on the mean for these two years are plotted on the right, with the mean value added alongside. The mean linear trend estimate (dashed line) and the one-standard deviation uncertainty are also provided.
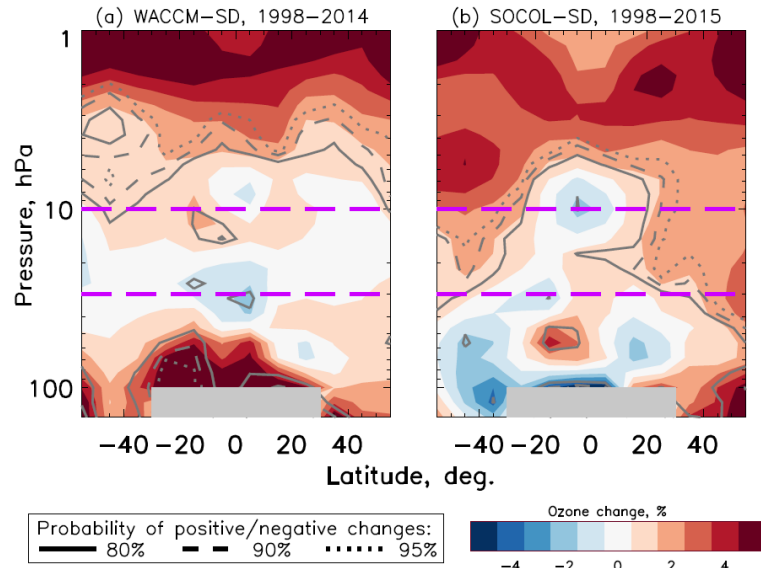
Figure 5: As for Fig. 1, but for (a) WACCM-SD and (b) SOCOL-SD.
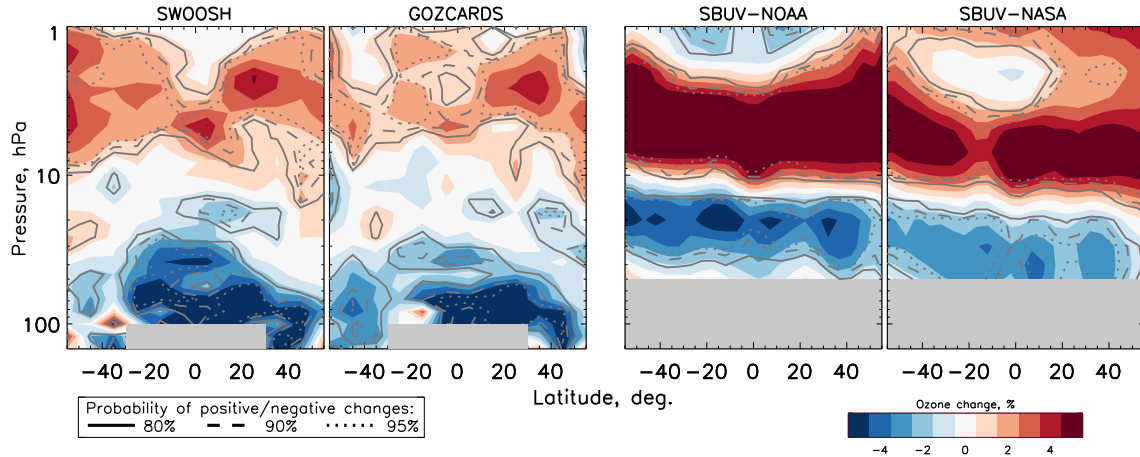
Figure A1: 1998-2016 ozone change. As for Fig. 1; from left to right, SWOOSH, GOZCARDS, SBUV-NOAA, and SBUV-NASA composites.
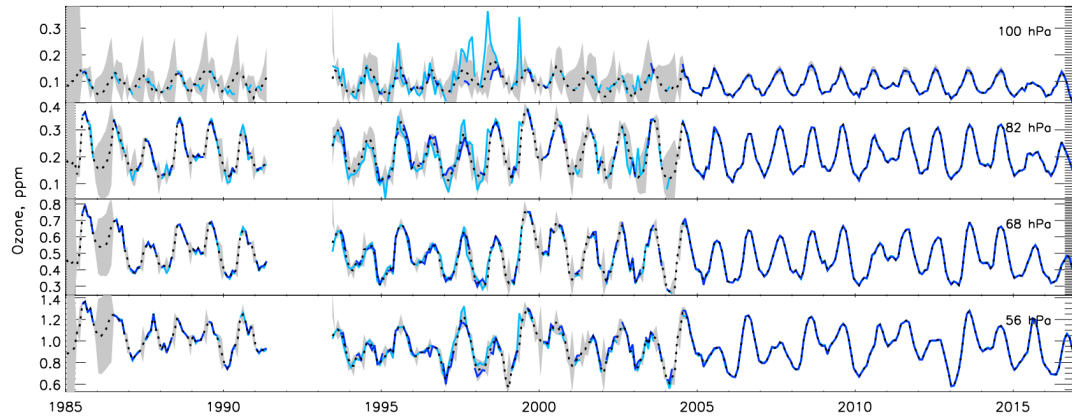
Figure A2: Example results of the merging procedure detailed in Ball et al. (2017) applied to GOZ-CARDS (dark blue), SWOOSH (light-blue) ozone composites in the 0-10°N band at four pressure levels indicated in the top right of each panel. The resulting Merged-SWOOSH/GOZCARDS time-series is shown as a dashed-black line with two standard deviation uncertainty in grey shading.
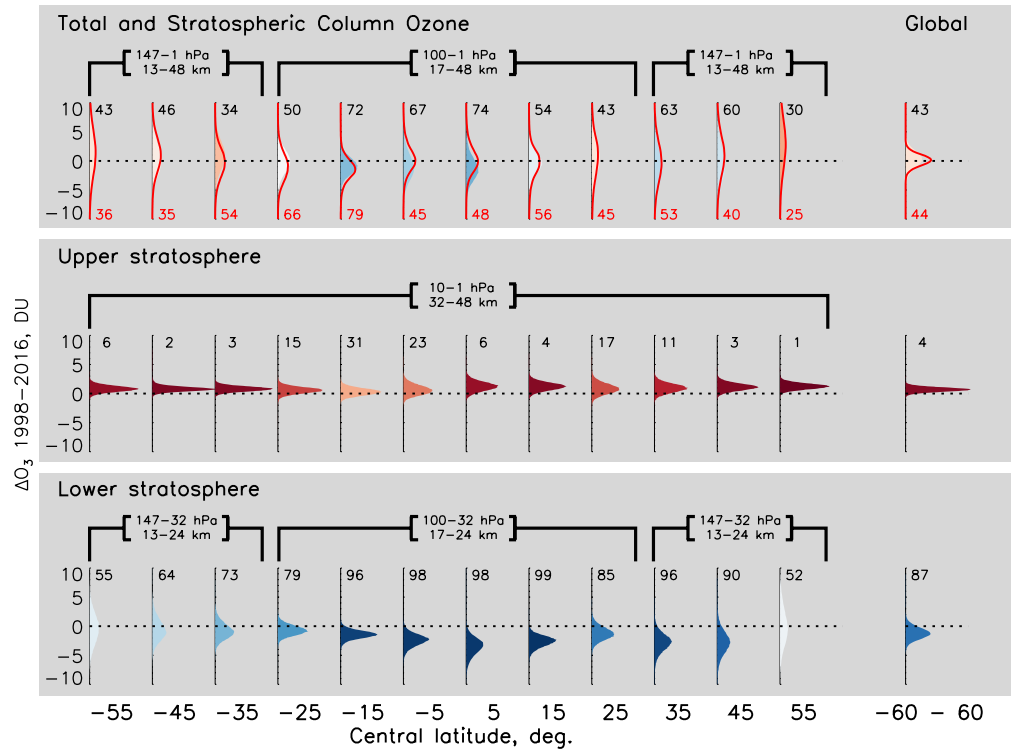
Figure A3: SAGE-II/OSIRIS/OMPS posterior distributions for the 1998-2016 ozone changes. See caption of Fig. 2 for details.
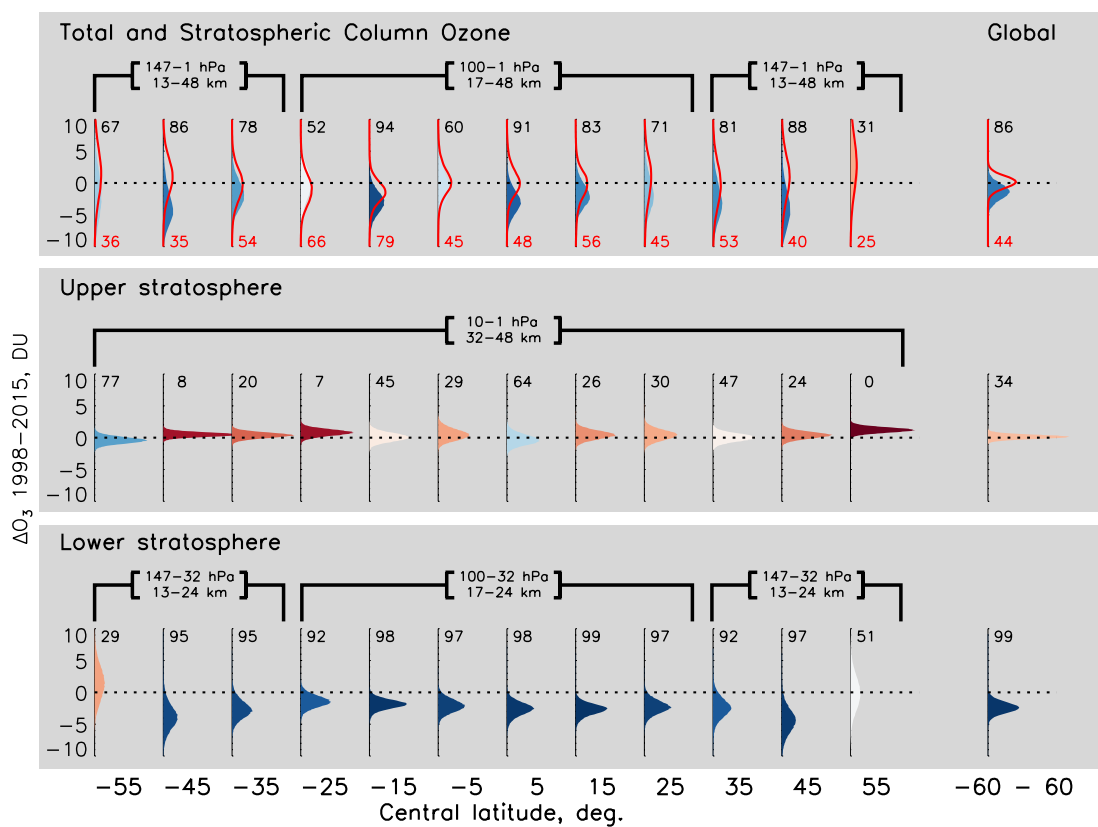
Figure A4: SAGE-II/CCI/OMPS posterior distributions for the 1998-2015 ozone changes. See caption of Fig. 2 for details.
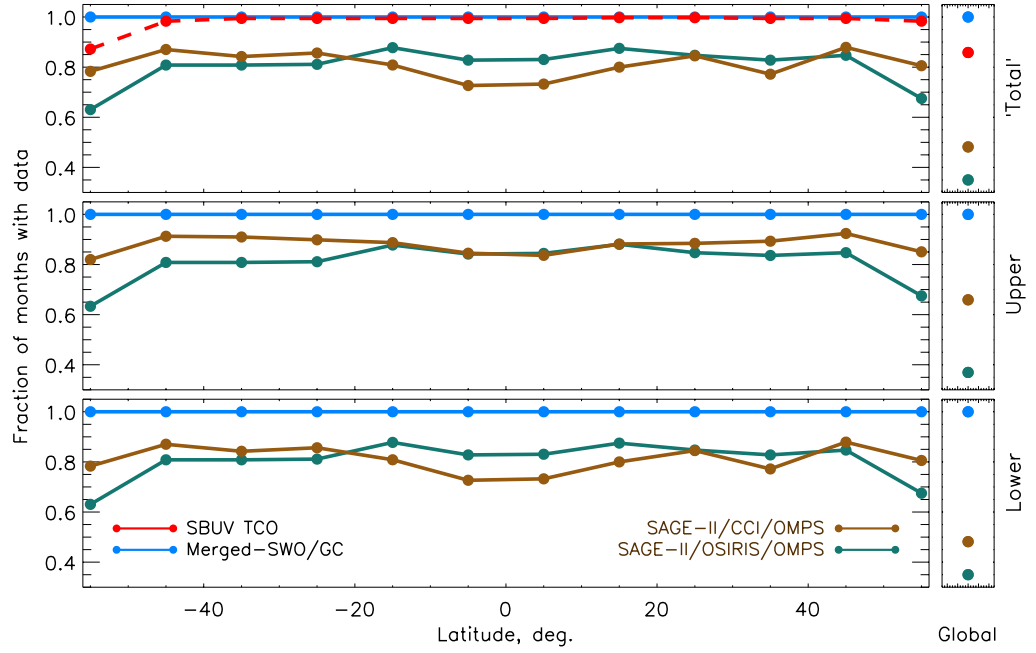
Figure A5: The fraction of data available for the (top) stratospheric column ozone and total column ozone, (middle) upper stratosphere, and (bottom) lower stratosphere posterior estimates in Figs. 2, A3, and A4. Global (right) are much lower in SAGE-II/OSIRIS/OMPS and SAGE-II/CCI/OMPS because if data are missing in any latitude in a particular month, the global partial column or stratospheric column ozone is assigned no data.
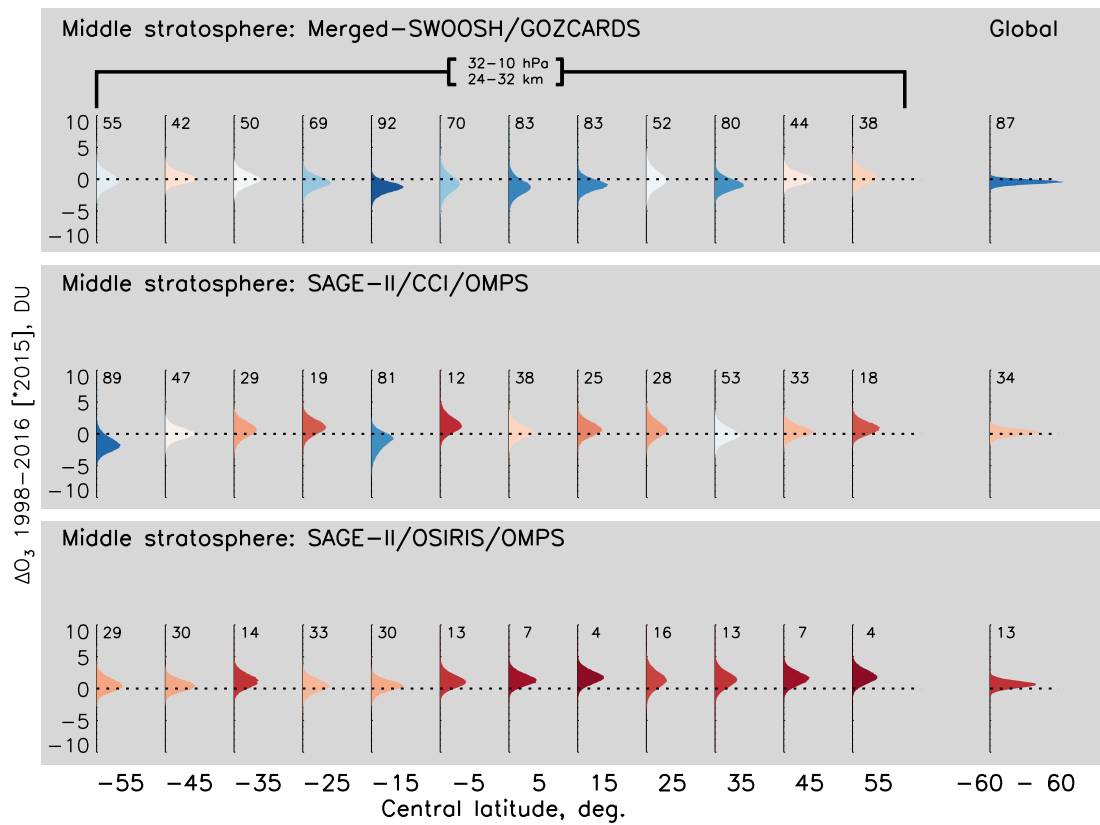
Figure A6: Posterior distributions in the middle stratosphere for the 1998-2015/2016 ozone changes. Similar to panels in Fig. 2, but for the middle stratosphere (32-10 hPa, ~24-32 km) for (top) Merged-SWOOSH/GOZCARDS, (middle) SAGE-II/CCI/OMPS, and (bottom) SAGE-II/OSIRIS/OMPS.
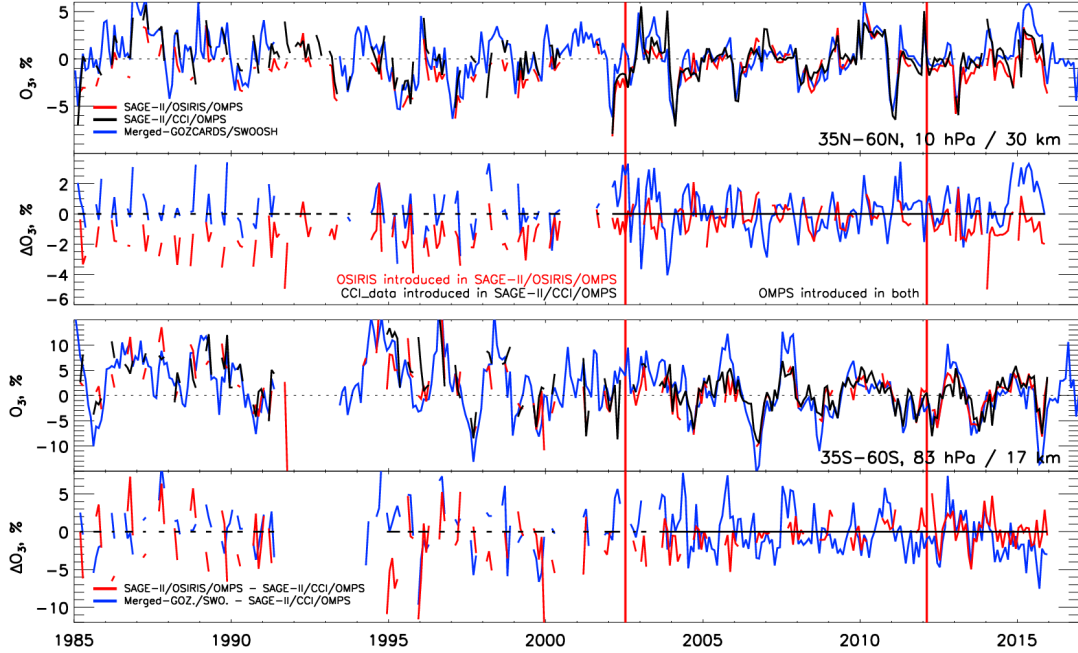
Figure A7: SAGE-II/OSIRIS/OMPS (red), SAGE-II/CCI/OMPS (black) at 30 and 17 km (upper and lower pair, respectively), and Merged-SWOOSH/GOZCARDS (blue) at pressure levels of approximately the same altitudes at 10 and 83 hPa, respectively. The upper panel of each pair shows the deseasonalised changes relative to 2005–2013, and the lower panel shows SAGE-II/OSIRIS/OMPS and Merged-SWOOSH/GOZCARDS relative to (i.e. minus) SAGE-II/CCI/OMPS. Approximate dates when OSIRIS and OMPS were introduced into the composites are shown with vertical red lines, before/after which a shift in the mean appears.
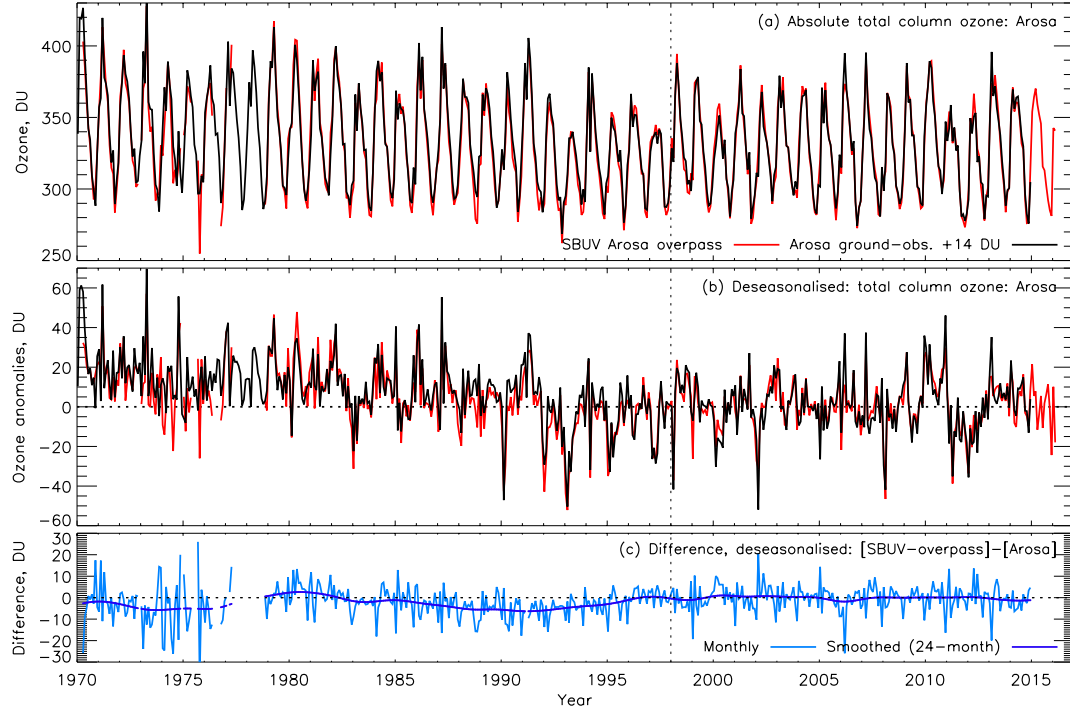
Figure A8: Ozone over Arosa, Switzerland, 1970-2016. (a) Absolute ozone from SBUV total column ozone overpass observations (red) compared to the ground-based Arosa total column ozone observations (black), with Arosa shifted to the SBUV mean for 1998-2013; (b) as for (a) with the seasonal cycle removed; (c) the monthly difference between timeseries in (b) and a 24-month Gaussian smoothing (thick line).
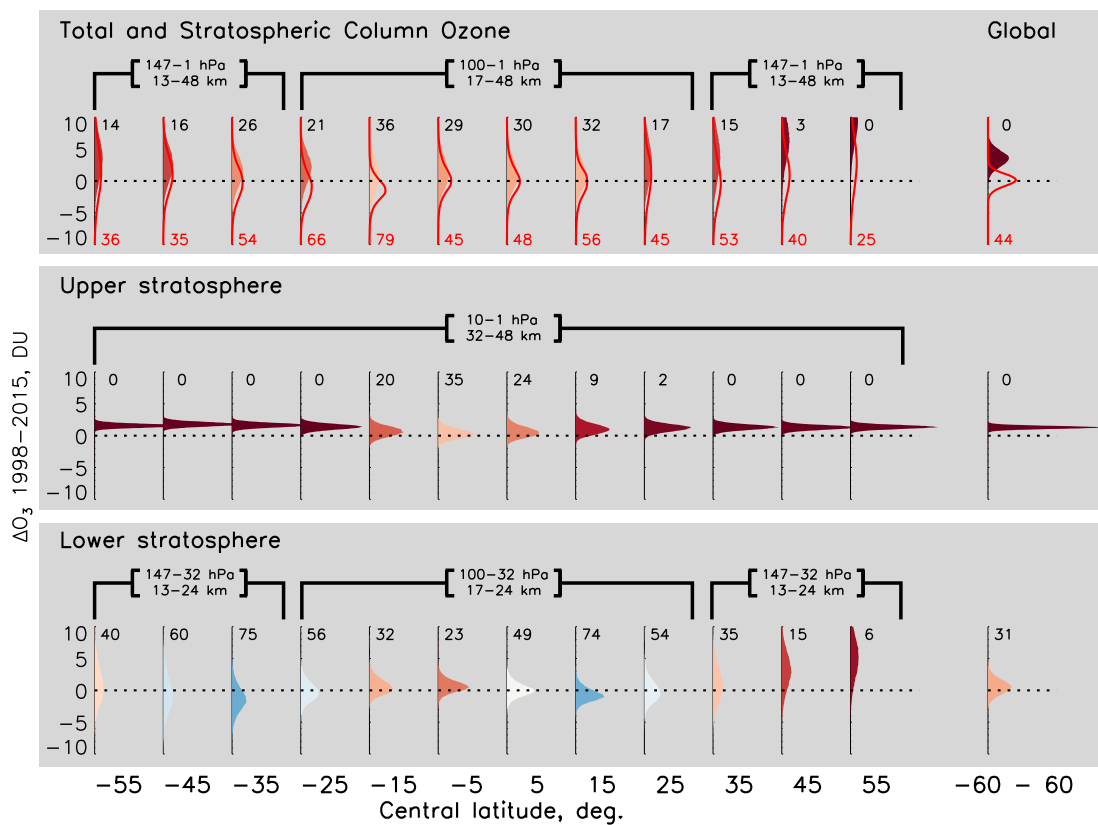
Figure A9: SOCOL-SD posterior distributions for the 1998-2015 ozone changes. See caption of Fig. 2 for details.
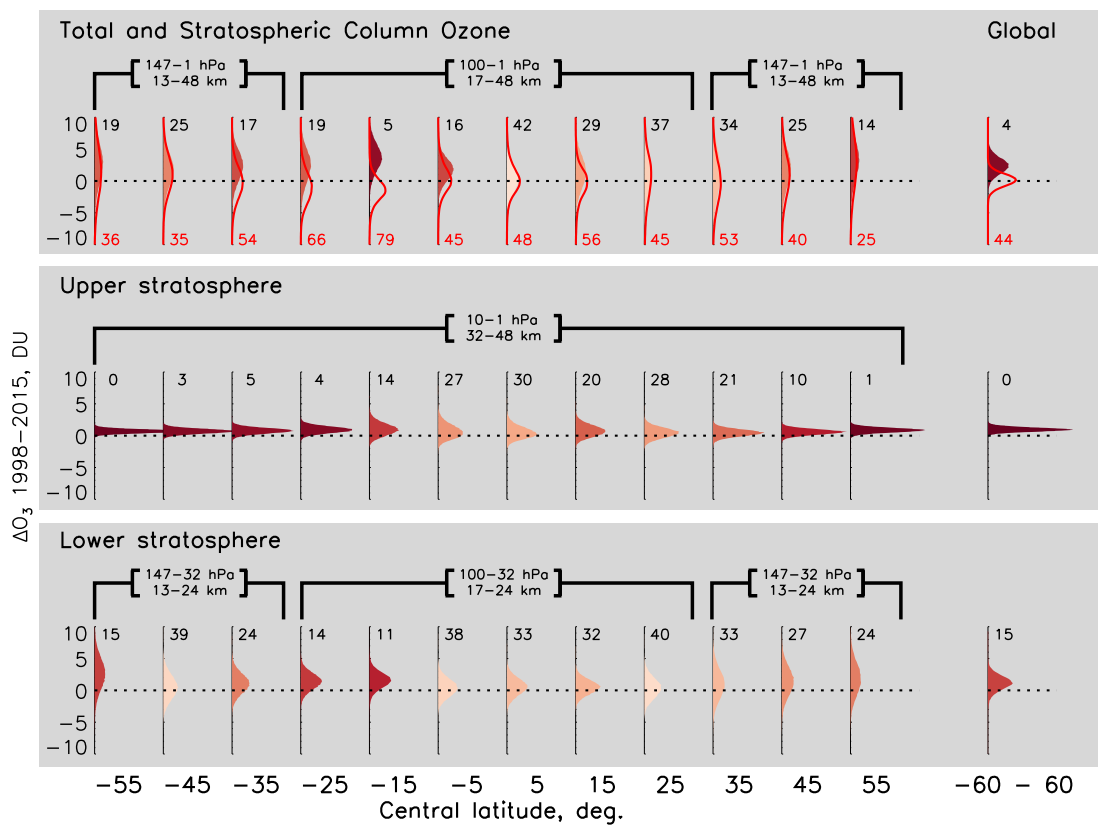
Figure A10: WACCM-SD posterior distributions for the 1998-2014 ozone changes. See caption of Fig. 2 for details.
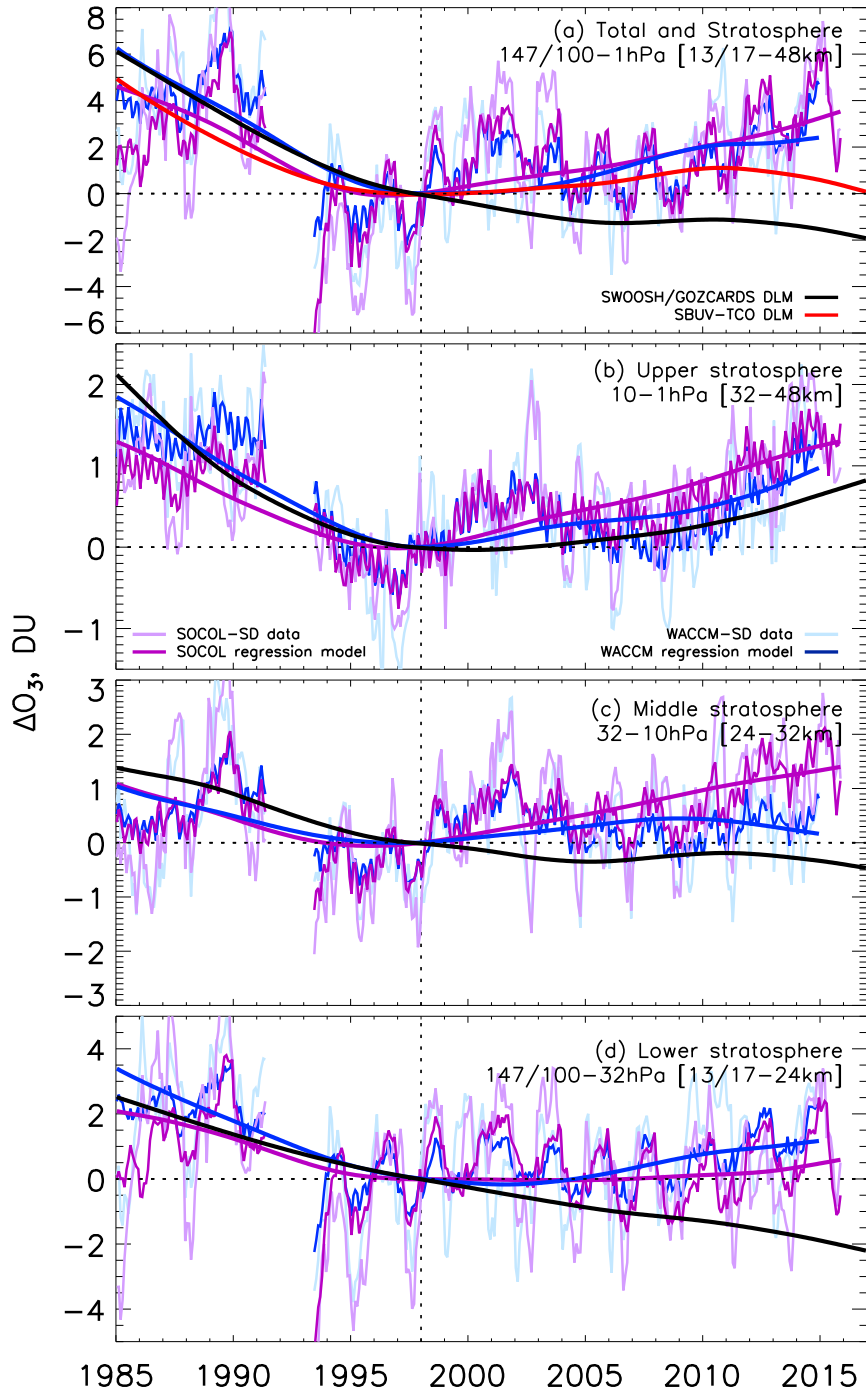
Figure A11: As for Fig. 3, but with deseasonalised and regression model timeseries from SOCOL-SD (purple) and WACCM-SD (blue). DLM results for SBUV total column ozone and Merged-SWOOSH/GOZCARDS are retained in this plot from Fig 3; see Fig 3 for more details.
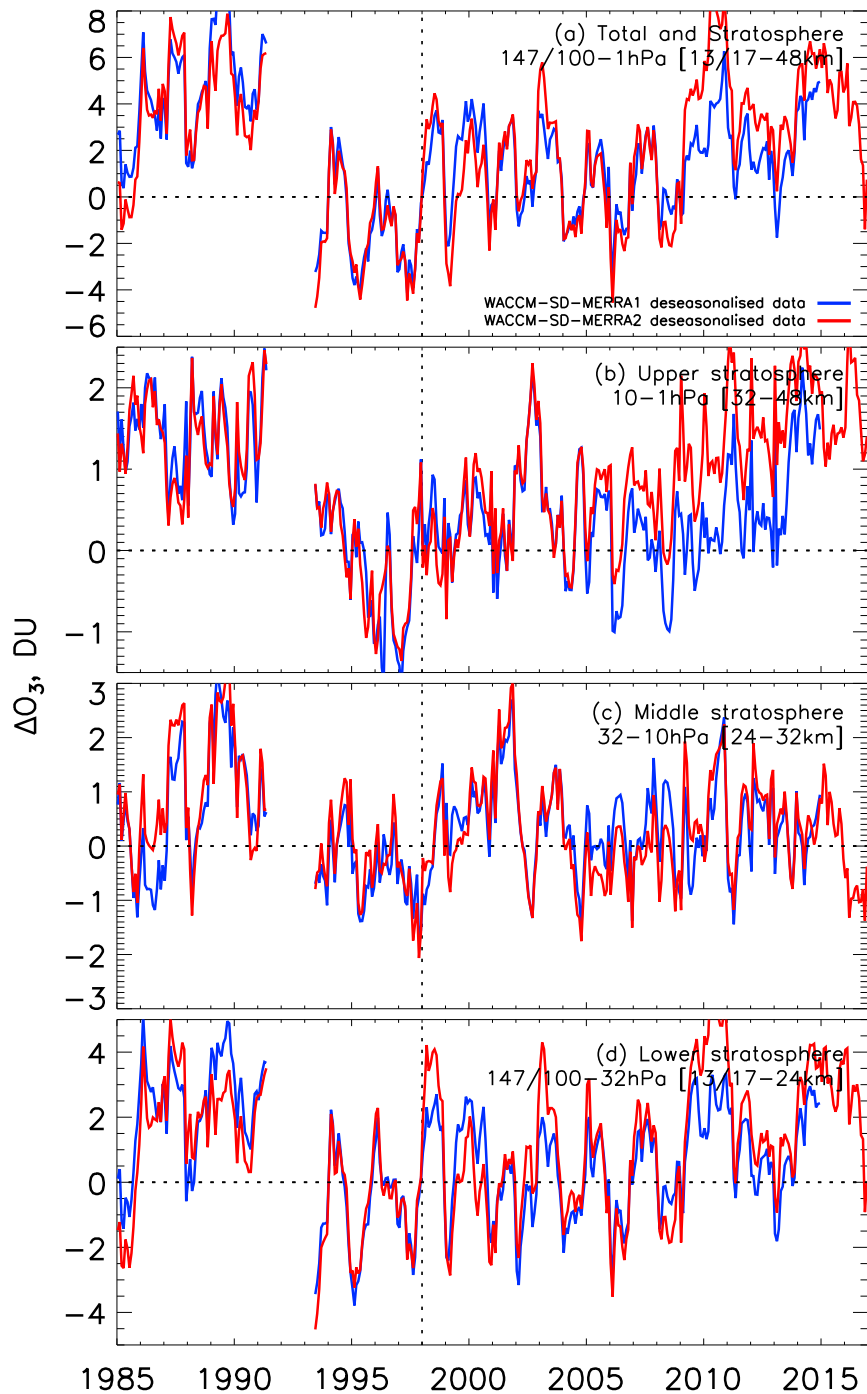
Figure A12: As for Fig. 3 and A11, but with deseasonalised model timeseries only from WACCM-SD using MERRA-1 (blue) and MERRA-2 (red).
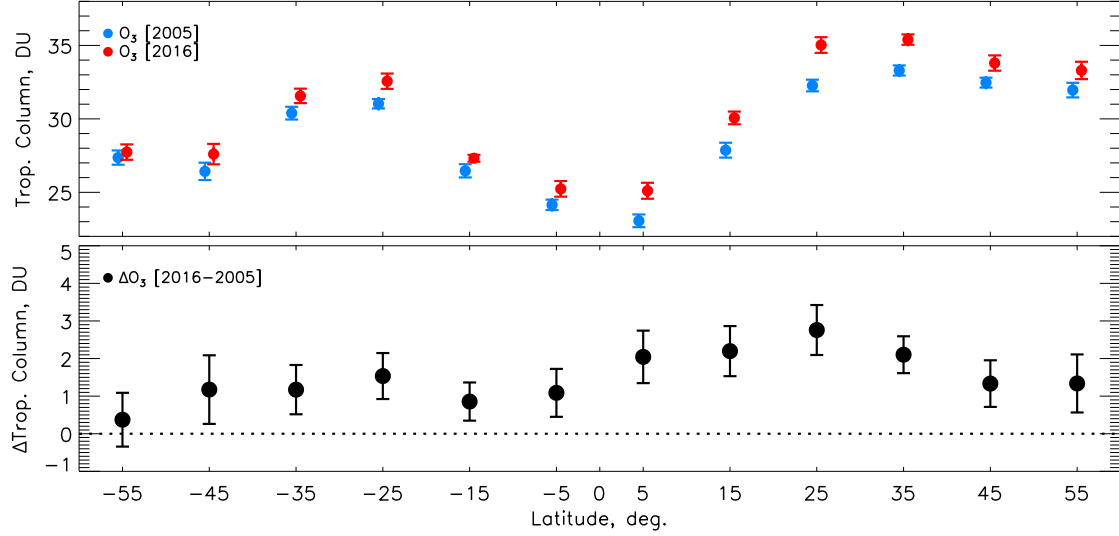
Figure A13: Mean and two standard errors of tropical column ozone change between 2005 and 2016 from OMI/MLS. The upper panel shows the absolute levels in 10° latitude bins in 2005 (blue) and 2016 (red), while the lower panel gives the difference between 2005 and 2016 with combined errors, similar to the right panel of Fig. 4.